



# Adaptive phenotypic plasticity is under stabilizing selection in *Daphnia*

Dörthe Becker<sup>1,2,3</sup>✉, Karen Barnard-Kubow<sup>1,4</sup>, Robert Porter<sup>1</sup>, Austin Edwards<sup>1,5</sup>, Erin Voss<sup>1,6</sup>, Andrew P. Beckerman<sup>1,2</sup> and Alan O. Bergland<sup>1</sup>✉

The adaptive nature of phenotypic plasticity is widely documented. However, little is known about the evolutionary forces that shape genetic variation of plasticity within populations. Whether genetic variation in plasticity is driven by stabilizing or diversifying selection and whether the strength of such forces remains constant through time, remain open questions. Here, we address this issue by assessing the evolutionary forces that shape genetic variation in antipredator developmental plasticity of *Daphnia pulex*. Antipredator plasticity in *D. pulex* is characterized by the growth of a pedestal and spikes in the dorsal head region upon exposure to predator cue. We characterized genetic variation in plasticity using a method that describes the entire dorsal shape amongst >100 *D. pulex* strains recently derived from the wild. We observed the strongest reduction in genetic variation in dorsal areas where plastic responses were greatest, consistent with stabilizing selection. We compared mutational variation ( $V_m$ ) to standing variation ( $V_g$ ) and found that  $V_g/V_m$  is lowest in areas of greatest plasticity, again consistent with stabilizing selection. Our results suggest that stabilizing selection operates directly on phenotypic plasticity in *Daphnia* and provide a rare glimpse into the evolution of fitness-related traits in natural populations.

Organisms frequently experience temporal and spatial fluctuations in their natural habitats. The capacity to persist and thrive across variable environmental conditions requires adaptation, either via allele frequency change or phenotypic plasticity. Phenotypic plasticity, the ability of a single genotype to express different phenotypes in response to altered environmental conditions, is ubiquitous in natural populations and well established as an adaptive response to fluctuations in the environment<sup>1,2</sup>. This adaptive response can provide time for a population to become established, reducing the probability of extinction in new or fluctuating environments<sup>3,4</sup> and also enables populations to efficiently traverse fitness landscapes<sup>5</sup>. Decades of theoretical and empirical work on the quantitative genetics of plasticity has revealed that genetic variation for plasticity exists<sup>5,6</sup>, that heritable variation in plasticity can respond to natural selection<sup>1,7</sup> and that plasticity can be both maladaptive<sup>8</sup> and subject to local adaptation<sup>9</sup>.

The adaptive nature of phenotypic plasticity has been demonstrated for behavioural, morphological and life-history traits<sup>10</sup>. Broadly, this work is aligned with theoretical predictions that adaptive phenotypic plasticity evolves when environmental change is rapid<sup>11,12</sup>, environmental cues are reliable<sup>13,14</sup>, plastic responses occur as rapidly as environmental change<sup>15</sup> and when the incurred cost of plasticity is low<sup>16,17</sup>. Empirical studies on the adaptive nature of phenotypic plasticity often measure aspects of fitness following environmental exposures (for example, ref. <sup>18</sup>) or document the plastic responses of genotypes collected from different locations that reflect alternate historical selection regimes (for example, ref. <sup>19</sup>). However, such data and insights do not reveal the selective forces shaping levels of genetic variation in plasticity within populations.

Distinct evolutionary forces remove and promote functional genetic variation within populations. On the one hand, theoretical models aimed at explaining the level of quantitative genetic diversity

in natural populations frequently highlight the central role of stabilizing selection<sup>20,21</sup>. Stabilizing selection reduces deleterious genetic variation in a population without modifying the population mean and maintains populations near their local fitness peak. Likewise, directional selection can reduce variation as populations adapt to a new fitness peak or evolve via genetic accommodation<sup>22,23</sup>. On the other hand, diversifying forces, including genetic overdominance, environmental heterogeneity and frequency-dependent selection, can maintain functional genetic variation<sup>24</sup>.

Whether stabilizing or diversifying forces predominate in natural populations and whether the strength of these forces remains constant through time, has remained one of the central challenges in evolutionary biology<sup>25</sup>. To test hypotheses about these forces that shape the magnitude of genetically based phenotypic diversity, both standing genetic variation ( $V_g$ ; for example, refs. <sup>13,26</sup>) and variation entering the population via mutations (mutational variation,  $V_m$ ; for example, refs. <sup>26,27</sup>) need to be considered<sup>28</sup>. Obtaining such data can be challenging and there is a pronounced data deficit in phenotypic plasticity research because of the challenge of measuring genetic variation across multiple environments. Consequently, there is a major gap in knowledge about the evolutionary forces that shape levels of standing genetic variation of plasticity within populations.

We directly address this gap in knowledge by evaluating signatures of natural selection on predator-induced morphological changes in the eco-evolutionary model organism, *Daphnia pulex*. This species responds to cues released from *Chaoborus* larvae by developing a morphological defence characterized by a pedestal protrusion and spikes on their dorsal head region<sup>29</sup>. This is a century old, classic example of adaptive phenotypic plasticity<sup>29–31</sup>. While development of morphological defences in *D. pulex*, which are typically maximized at second and third juvenile instars (for example, refs. <sup>29,31–33</sup>), increases survival to predator attack by up to 50%

<sup>1</sup>Department of Biology, University of Virginia, Charlottesville, VA, USA. <sup>2</sup>School of Biosciences, Ecology and Evolutionary Biology, University of Sheffield, Sheffield, UK. <sup>3</sup>Department of Biology, University of Marburg, Marburg, Germany. <sup>4</sup>Department of Biology, James Madison University, Harrisonburg, VA, USA. <sup>5</sup>Biological Imaging Development CoLab, University of California San Francisco, San Francisco, CA, USA. <sup>6</sup>Department of Integrative Biology, University of California Berkeley, Berkeley, CA, USA. ✉e-mail: [d.becker@sheffield.ac.uk](mailto:d.becker@sheffield.ac.uk); [aob2x@virginia.edu](mailto:aob2x@virginia.edu)

(refs. <sup>29,33</sup>), induction in the absence of actual predators incurs a fitness cost<sup>29,30</sup>. Surveys of natural populations have shown that induction in wild individuals is positively correlated with *Chaoborus* density<sup>34</sup> and experimental exposure with *Chaoborus* extract produces the same induction as seen in wild-caught individuals<sup>34</sup>. Therefore, the antipredator morphological defences expressed in juvenile instars of *D. pulex* are probably subject to strong selection and provide a tractable system to study the evolutionary forces acting on phenotypic plasticity.

Modes of selection—those that remove fitness-related variation (stabilizing and directional) and those that maintain it (diversifying)—are likely to leave distinct signatures of standing genetic variation. If stabilizing selection acts strongly on the plastic inducible defence, we predict that genetic variation in dorsal shape will be reduced upon exposure to predator cue relative to genetic variation in dorsal shape in the absence of predator cue. Moreover, we predict that the dorsal regions that show the greatest plasticity will show the greatest reduction of variation in the predator cue treatment. This prediction is based on the idea that the strength of selection on aspects of dorsal shape will be stronger in the presence of predators versus the absence of predators. In addition, we also predict that if stabilizing selection acts strongly on the plastic response, the ratio of additive genetic variation to mutational variation ( $V_g/V_m$ ) in the induced state will be lowest in dorsal regions that show the greatest plasticity, relative to the rest of the dorsal edge of the organism. Alternatively, diversifying selection could operate on the plastic response if, for instance, the strength or type of predation varies across microhabitats or through time. If diversifying selection is a prominent feature, we expect that genetic variation in dorsal shape will be large upon exposure to predator cue relative to genetic variation in dorsal shape in the absence of predator cue. Thus, in contrast to the above, we predict that diversifying selection should increase genetic variation in dorsal regions that show the greatest plasticity, relative to the rest of the dorsal edge of the organism.

To evaluate these alternative predictions, we combined a high-throughput phenotyping assay with genome resequencing to characterize the evolutionary forces acting on plastic induction. We first show that standing genetic variation for the defence, in an outbred population, is reduced upon exposure to predator cue. This reduction of genetic variation is greatest in the dorsal head region where defence morphologies are expressed. We also demonstrate statistically that this head region is a discrete phenotypic module and thus likely to respond to selection independently from the surrounding dorsal regions. We next measured mutational variation in defence morphologies using strains that are clonally related and have accumulated new mutations in the wild since they diverged from their recent common ancestor<sup>35</sup>. Among-line variation thus reflects mutational variation ( $V_m$ ; refs. <sup>28,36–38</sup>) and can be contrasted to standing variation ( $V_g$ ) in the outbred individuals. Consistent with the view that the environmentally induced phenotype is subject to stabilizing selection, we show that  $V_g/V_m$  is lowest in the phenotypic module that showed greatest phenotypic plasticity. Taken together, these data provide unique insight into the evolution of environmentally induced, plastic responses and the forces that shape genetic variation in the wild.

## Results

**Robust and accurate phenotyping.** To date, assessment of predator-induced morphological changes in *Daphnia* have been based on a categorical scoring technique that classifies pedestals as absent (score = 0), small (score = 30) or large (score = 50) and neckteeth in increments of ten<sup>29,33</sup>. Although this scoring technique has been useful, its coarse scale and potential for observer bias limits our capacity to assess morphological responses with high resolution, replication and reproducibility.

To remedy this, we developed a phenotyping tool, DAPCHA, that allows automated identification of defined phenotypic landmarks and subsequent quantification of phenotypic responses using standardized photographic images from stereoscope microscopy (Fig. 1a). These features include basic aspects of morphology such as animal length, eye size and tail length (Fig. 1a,ii), as well as a trace of the entire dorsal edge central to detecting the induced defences (Fig. 1a,iii). DAPCHA accurately measures animal length (Fig. 1b; Pearson's correlation:  $r(707) > 0.99$ ,  $P < 2.2^{-16}$ ; Supplementary Table 1, section I) and is more repeatable in unit conversion of length estimates than are manual observers (for example, run 2, Fig. 1c and Supplementary Table 1, section I).

We used DAPCHA to calculate the maximum dorsal height of the animal (Fig. 1a, V and Methods) as a summary of morphological responses before and after exposure to predator-derived kairomones. We find that maximum dorsal height is an excellent proxy for the predator cue-induced morphological defence (Wilcoxon rank sum test:  $Z = -7.79$ ,  $P = 6.558^{-15}$ ; Supplementary Table 1, section I) and is also correlated with estimates of defence based on the discrete manual scale (Fig. 1d, predation; Pearson's correlation:  $r(240) = 0.4$ ,  $P = 6.291^{-11}$ ; Supplementary Table 1, section I). We also show low consistency in manual assessment of the pedestal score among three independent observers: only 66% and 74% of individuals were classified as the same induction level during instar 1 and instar 2, respectively, when exposed to predator cues (Extended Data Fig. 1 and Supplementary Table 1, section IV). These data suggest that DAPCHA is a useful approach to assess phenotypic responses in a consistent manner. We retroactively assigned animals to the first instar and second instar (Fig. 1e) on the basis of a multimodal distribution of animal length and animal dorsal area (Methods), enabling us to ask questions about the extent of morphological response in distinct size and age classes.

**Evidence for stabilizing selection in an outbred sample.** We estimated components of phenotypic variation in the environmentally induced, plastic response of 471 individuals from among 49 genetically unique strains (Extended Data Fig. 2 and Supplementary Table 2) sampled from a single population in southern England<sup>35</sup>. We reared each strain with and without predator kairomone and applied our DAPCHA pipeline to around four individuals per strain and treatment group each day, for the first 3–4 d postparturition (Extended Data Fig. 3).

First, we evaluated the plastic response of these strains. We demonstrate that exposure to predator kairomone induces defence morphologies, most prominently in the dorsal head region (Fig. 2a,e and Extended Data Fig. 4). The magnitude and position of the induced pedestal varied between predator cue exposed and control individuals. Under predation risk, the maximum dorsal height shifted towards anterior head regions (Fig. 2a,b and Extended Data Fig. 4; Chi-squared test (instar 2):  $\chi^2[\text{d.f.} = 112, n = 380] = 222.4$ ,  $P = 2.676^{-9}$ ; Supplementary Table 1, section II) and the maximum dorsal height increased (Fig. 2c; Wilcoxon rank sum test (instar 2):  $Z = -9.84$ ,  $P < 2.2^{-16}$ ; Supplementary Table 1, section II). Furthermore, we detected an increase in the number of neckteeth upon exposure to predator cue (Fig. 2d; Chi-squared test (instar 2):  $\chi^2[\text{d.f.} = 7, n = 381] = 179.83$ ,  $P < 2.2^{-16}$ ; Supplementary Table 1, section II).

A quantitative genetic test of modularity<sup>39–41</sup> (Methods) indicates that phenotypic responses in the dorsal head region (module 2), where defences are expressed, are expressed independently of, and do not covary with, any change in the rest of the body plan (covariance ratio coefficient (instar 2): CR = 0.72,  $P = 0.001$ ; Extended Data Fig. 5, model H). This finding suggests that the dorsal head region (between dorsal positions 100 and 200; Extended Data Fig. 5, model H) is a phenotypic module that probably responds to natural selection independently of the rest of the body plan.

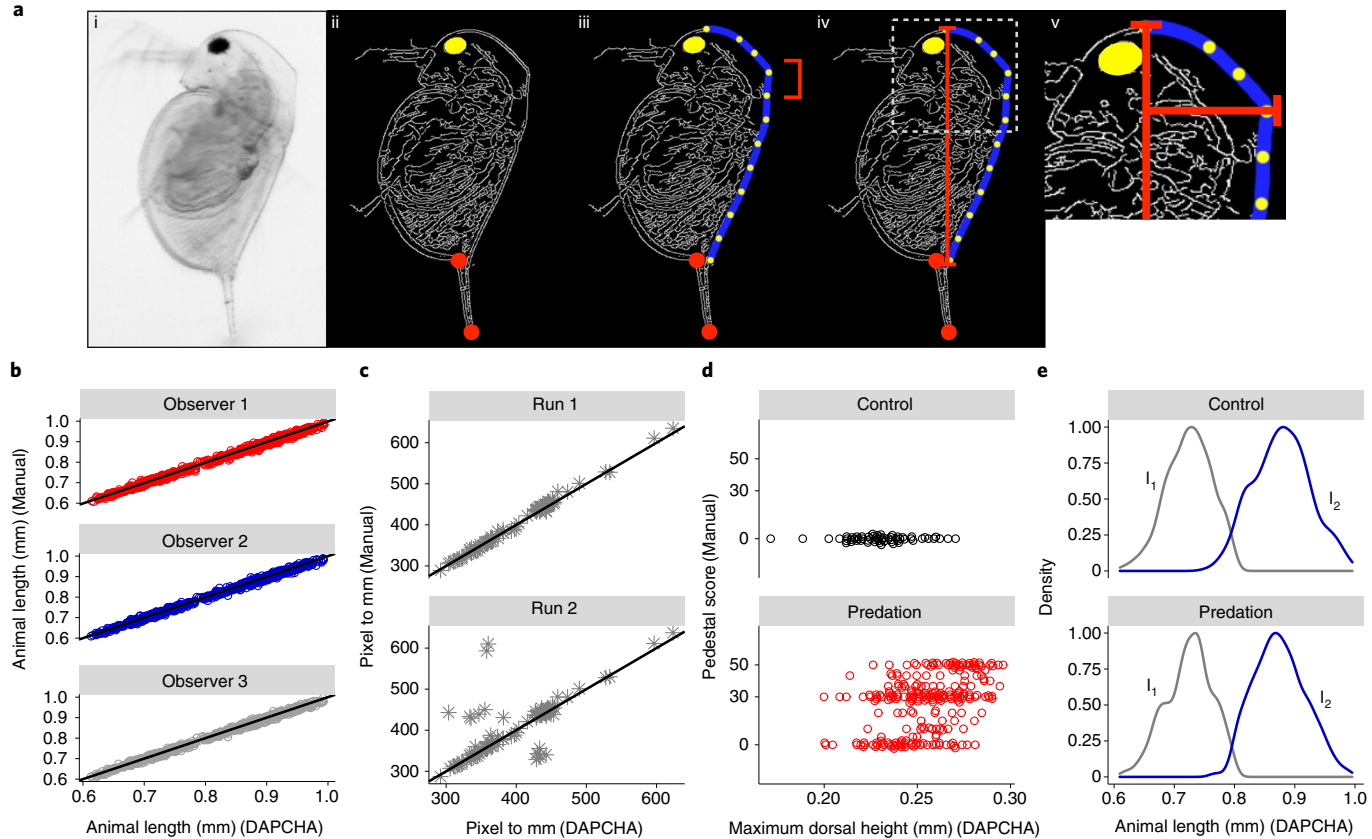


**Fig. 1 | High-throughput phenotypic assessment via automated image analysis tool DAPCHA.** **a**, Phenotypic assessment of *Daphnia* using DAPCHA involves three major steps: conversion of a standardized, raw image to grayscale (i and ii); automated identification of key landmarks (eye, tail tip and tail base) (ii); and automated tracing of the dorsal edge of the carapace (blue line) via identification of equally spaced landmarks along the dorsal axis. In total, we used 600 dorsal positions; yellow points in the figure highlight major landmarks (iii). Defined landmarks subsequently allow for the quantification of different phenotypic traits, including animal length (iv) and dorsal height (v; here exemplified by the dorsal position where dorsal height was largest). **b-d**, Accuracy of phenotypic estimates by DAPCHA were validated via contrasting manual estimates with automated data: animal length estimates across three different observers (**b**); unit conversion of length estimates using a microstage meter with manual estimates assessed in two different runs (Methods) (**c**); and morphological changes in the head region (square bracket in **a**, iii) under control and predation conditions in second instar animals; manual scores are averaged across three independent observers giving rise to values other than 0, 30 and 50 (**d**). **e**, Using a mixture model on animal length and animal dorsal area, test animals were retroactively assigned to distinct developmental stages (first instar,  $I_1$ ; second instar,  $I_2$ ).

Next, we decomposed phenotypic variation among the outbred individual lines to estimate the relative contribution of genotype, environment and genotype-by-environment interaction ( $G \times E$ ) at each position along the dorsal axis (Fig. 2a). We observe a strong environmental effect on dorsal height among our outbred strains (Fig. 2e, red line and Supplementary Table 1, section II) with the peak of morphological induction centred in the independent head module (around dorsal position 150 in module 2; Extended Data Fig. 5, model H). We further observed substantial genetic variation in the induced morphological defence (Fig. 2e, blue line and Supplementary Table 1, section II).

The data indicate an increase in  $G \times E$  variation for second instar animals in module 2 (Extended Data Fig. 5, model H), with effect sizes up to 16% higher in this module than effect sizes averaged across other body parts (Fig. 2e, grey line). This elevated  $G \times E$  near the region of maximum induction could be caused by crossing reaction norms or by a change in genetic variance between the control and predator cue environments. To test these alternative explanations, we calculated both the broad- and narrow-sense heritability of dorsal height in the control and predator-induced environments. In second instar animals, we find a reduction of both measures of heritability for dorsal height upon exposure to predator cue

(Fig. 2f-h and Supplementary Table 1, section II), with the strongest reduction in heritability estimates upon exposure to predator cue in module 2 (Extended Data Fig. 5, model H; Wilcoxon rank sum test (instar 2, module 2):  $Z = -9.15$ ,  $P < 2.2^{-16}$ ; Supplementary Table 1, section II). This result is consistent with the hypothesis that the induced phenotype is subject to stabilizing selection.

**Mutational variation and further evidence of stabilizing selection.** We contrasted levels of standing genetic variation ( $V_g$ ) with mutational variation ( $V_m$ ) to further evaluate evidence for stabilizing versus diversifying evolutionary forces. To estimate mutational variation in the plastic response, we assayed 516 individuals from among 56 clonally related strains (Extended Data Fig. 2 and Supplementary Table 2). These clonally related strains show genetic high similarity but differ due to new mutations (collectively including point mutations, small indels, gene conversion) that have arisen as the clonally related individuals that we measured shared a common ancestor<sup>35</sup>. These clonally related strains were independently isolated from the field and sampled from the same set of ponds at the same time as the outbred individuals above, allowing us to directly relate levels of genetic variation in the induced phenotype. All experimental work with these clonally related strains was done

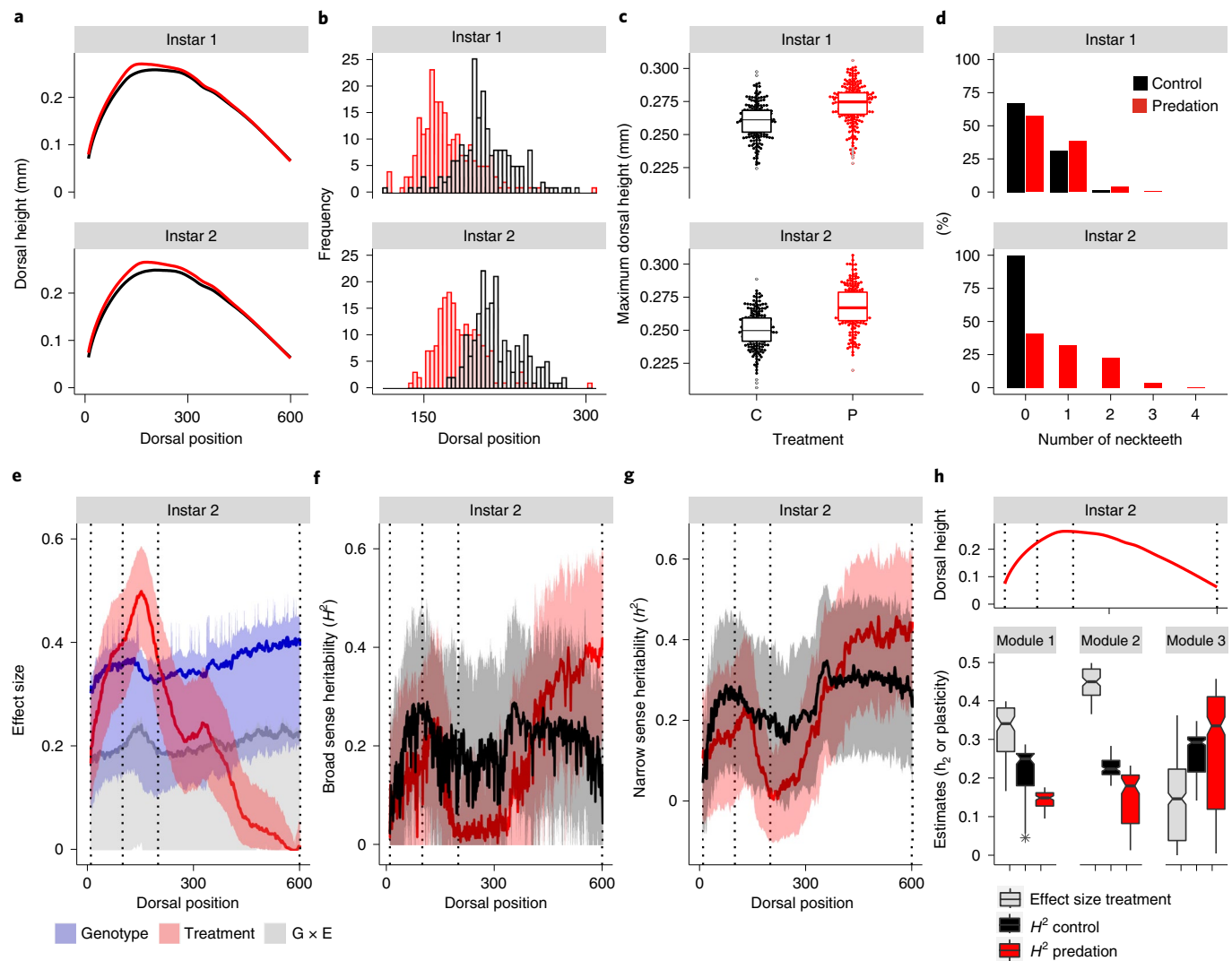


**Fig. 2 | Effects of predation risk on morphological changes in genetically unique strains.** **a**, Risk of predation induces marked shape changes along the dorsal axis in first and second instar *D. pulex* (control, black line; predation, red line). **b**, Strongest morphological changes are observed in the head region, with maximal dorsal height shifting towards anterior head regions under predation risk. **c**, Predator-induced defence morphologies, here measured as maximal dorsal height, increase in response to predation risk exposure in both instars (control (C), black points; predation (P), red points). **d**, The number of neckteeth increases in response to predator cue, particularly in second instar animals. **e**, Effect sizes from a linear model along the dorsal axis reveal distinct patterns of treatment (predation risk, red line), genotype (blue line) and  $G \times E$  interaction (grey line) effects on morphological changes in second instar animals. **f,g**, Broad-sense (**f**) and narrow-sense (**g**) heritability estimates of dorsal height in second instar *Daphnia* vary along the dorsal axis in response to control conditions (black line) and predation risk (red line), with a strong reduction of both measures of heritability for dorsal height upon exposure to predator cues in the dorsal head region where defence morphologies are expressed (**a**, Fig. 1*a,iii*). Data in **e,f** and **g** are presented as mean values, with shaded areas indicating upper (0.95) and lower (0.05) confidence intervals. Vertical lines in **e,f** and **g** highlight morphological independent shape modules, separating head and posterior body areas (Extended Data Fig. 5). **h**, Boxplots of narrow-sense heritability estimates (see **g**; black, control; red, predation) and treatment effect sizes (see **e**) across the identified three independent shape modules (top panel) in second instar animals. Data in **c** and **h** are based on biologically independent samples:  $n=192$  (control,  $I_1$ ),  $n=220$  (predation,  $I_1$ ),  $n=193$  (control,  $I_2$ ),  $n=188$  (predation,  $I_2$ ).

using the same experimental design as described above and assayed concurrently with the genetically unique outbred lines (Extended Data Fig. 3). Population genomic analysis suggests that these clonally related isolates share a recent common ancestor and are also related to the outbred individuals that we studied here<sup>35</sup>.

These clonally related strains display a robust plastic response to predator cue that is similar to the average plastic response of the outbred individuals (Extended Data Fig. 6 and Supplementary Table 1, section VI). We also detected considerable variation in the induced defence morphologies among these clonally related strains in several key metrics of the induced phenotype such as the height along

the dorsal axis (Extended Data Fig. 6a and Supplementary Table 1, section VI) and the maximum height of the pedestal (Extended Data Fig. 6c and Supplementary Table 1, section VI).

We confirmed by performing a ‘twin analysis’ that the phenotypic variance that we observe among these clonally related strains is heritable and unlikely to be caused by other factors such as maternal effects or experimental artefact. This analysis takes advantage of our split-block experimental design in which, on average, eight strains were phenotyped concurrently across 20 batches in total (Methods). These batches were relatively evenly split between treatment groups and clonal and outbred individuals (Extended Data Fig. 7).

Specifically, we evaluated the correlation of the environmentally induced trait between siblings released from the same mother ('within clutch') and between individuals from the same strain but born to different mothers ('within clone'), replicated across the 56 strains of the same clonal assemblage (genetically similar strains; Extended Data Fig. 3 and Supplementary Table 2). If the statistically significant among-line variance (Extended Data Fig. 6e, Supplementary Table 1, section VI) that we observe across the clonally related strains was due to experimental artefact or shared environmental batch effect, the correlation between individuals released from the same mother ('twins' and 'within clutch') will be higher than the correlation between individuals released from different mothers of the same strain ('cousins' and 'within clone'). Similarly, if the among-line variance of the clonally related strains is due to experimental artefact, the correlation between individuals within a batch should be high.

On the other hand, if new mutations (or heritable epigenetic marks; for example, ref.<sup>42</sup>) cause phenotypic differentiation between clonally related strains, then twins should be (1) as similar to each other as cousins and (2) more similar to each other than to other genetically similar lineages of the clonal assemblage ('among clones').

In line with the expectation that mutations underlie the observed variation, we detected strong correlation between twins and between cousins and that these individuals are more similar to each other than to randomly paired individuals sampled across the clonal assemblage (Extended Data Fig. 8 and Supplementary Table 1, section VII). Moreover, the correlation coefficients between twins broadly exceeded the expectations from permutations (Extended Data Fig. 8, 'within clutch' and Supplementary Table 1, section VII), while correlations of randomly paired individuals from the clonal assemblage were markedly lower (Extended Data Fig. 8, 'within clutch' versus 'among clones' and Supplementary Table 1, section VII).

We also detected low correlations of phenotypic responses among randomly paired individuals from the same experimental batches (Extended Data Fig. 8, 'among batches' and Supplementary Table 1, section VII), suggesting that both experimental batch and maternal effects are not driving the observed variance among clonally related strains. This finding was further supported by fitting full linear mixed models, with variance components suggesting that most phenotypic variation is due to differences among clonally related strains but not due to batch effects or maternal effects ('max dorsal height', Supplementary Table 1, section VII).

From these analyses, plus the linear model approach in section 'Evidence for stabilizing selection in an outbred sample' (Fig. 2), we conclude that there are heritable differences in the environmentally induced phenotypic response between strains that are clonally related. We interpret this among-line variance as mutational variance,  $V_m$ . The magnitude of  $V_m$  that we document here is on par with estimates of mutational variance in other *Daphnia* studies<sup>43</sup>. The large mutational variance also demonstrates that plastic, environmentally induced responses are not mutation limited and suggests that local adaptation in the plastic response (for example, ref.<sup>9</sup>) could, in principle, be driven by new mutations that arise frequently.

To estimate the strength of stabilizing selection on the observed phenotypic responses in both the presence and absence of predator cue, we contrasted standing genetic variation ( $V_g$ ) with the mutational variance ( $V_m$ ) using the among-line variance of genetically unique strains and the among-line variance of clonally related strains, respectively. We detected that  $V_g/V_m$  is lowest in module 2 (Extended Data Fig. 5, model H) in second instar animals exposed to predator cue (Fig. 3a,b; Kruskal–Wallis rank sum test:  $\chi^2[{\rm d.f.}=2]=34.665$ ,  $P=2.969^{-8}$ ; Supplementary Table 1, section III). In addition, we find the strongest statistical support for a reduction in  $V_g/V_m$  upon exposure to predator cue in module 2

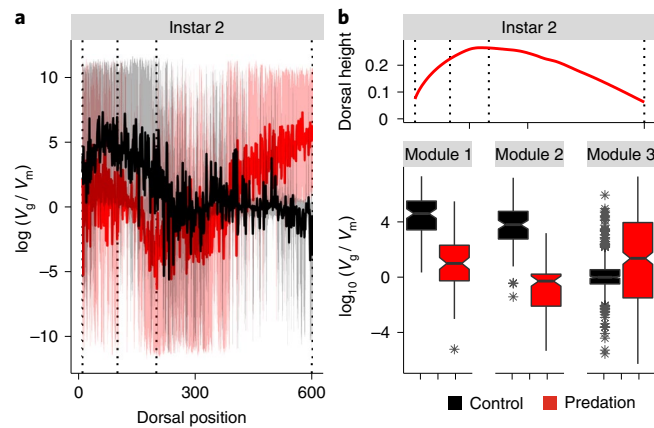


**Fig. 3 | Effects of natural selection on predator-induced plastic responses in second instar *Daphnia*.** **a**, The  $\log_{10}(V_g/V_m)$  estimates of dorsal height vary along the dorsal axis in response to control conditions (black line) and predator cue (red line). Notably, genetic diversity is strongly reduced in the dorsal head region of second instar *Daphnia* (module 2; Extended Data Fig. 5 and Supplementary Table 1, section III) upon exposure to predator cue (red line). Data are presented as mean values, with shaded areas indicating upper (0.95) and lower (0.05) confidence intervals. Vertical lines highlight morphological independent shape modules, separating head and posterior body areas (Extended Data Fig. 5). **b**, Boxplots of  $\log_{10}(V_g/V_m)$  estimates across the identified three independent shape modules (top panel) in second instar animals. Data in **b** are based on  $n=193$  (control) and  $n=188$  (predation) biological samples.

(Wilcoxon rank sum test (instar 2, module 2):  $Z=-11.35$ ,  $P<2.2^{-16}$ ; Supplementary Table 1, section III). The localized reduction of  $V_g/V_m$  (Fig. 3b,c), coupled with the reduction of  $V_g$  in the induced state (Fig. 2f–h), provides strong evidence for stabilizing selection operating on this environmentally induced trait.

## Discussion

We evaluated evidence about the role of stabilizing selection versus diversifying selection shaping phenotypic plasticity using estimates of standing genetic variation and mutational variation. We provide two lines of evidence to support a conclusion that stabilizing selection is acting on induced defences, a classic form of adaptive phenotypic plasticity. We show that standing genetic variation is reduced in phenotypic modules associated with the defence morphologies (Fig. 2) and we show that standing genetic variation in the induced phenotype is substantially lower than mutational variation (Fig. 3). Although the intuitive model that an environmentally induced phenotype is directly related to fitness forms the basis for a century of work studying the antipredator responses of *D. pulex*<sup>29,44</sup> and other related Cladocera<sup>45,46</sup>, to our knowledge, this idea has not been directly tested. Our work, therefore, provides new insight into the evolutionary history of plastic phenotypes.

Phenotypic plasticity is a vital strategy for organisms to cope with rapid changes in their environment<sup>1,12,15,47</sup> and prior research has demonstrated that aspects of phenotypic plasticity can evolve in response to changes in the environment<sup>3,4</sup>. Theoretical models that explain the evolution of plasticity assume that genetic diversity is sufficiently present<sup>48,49</sup> and this assumption is generally realized when examining empirical data in a wide variety of species (for example, ref.<sup>50</sup>). Despite the ubiquity of genetic variation in plasticity across the tree of life and genetically based phenotypic variation of fitness-related traits in general<sup>51</sup>, determining the evolutionary forces that act on that variation remains a fundamental challenge<sup>25</sup>. Determining the evolutionary history of phenotypic variation requires a comparative approach and often comparisons are made

between populations to study local adaptation<sup>9,18</sup> or across taxa to study diversification<sup>52,53</sup>. As a consequence, identifying the forces that shape genetically based phenotypic variation within populations remains relatively understudied.

To gain insight into the evolutionary determinants of phenotypic variation within populations, it is critical to understand the extent of mutational variance. Mutational variance is generally considered deleterious<sup>54</sup> and, therefore, the rate at which it is removed from populations should reflect the strength of purifying selection<sup>55</sup>. Although directly observing the trajectory of new mutations is challenging, as is disentangling genetic versus epigenetic inheritance in studies of mutational variance, comparisons of standing genetic variation to mutational variation can yield insight into the expected persistence time of new, deleterious mutations<sup>55</sup>, the mutational target size<sup>56</sup> and the genetic architecture of different classes of traits<sup>43</sup>. For instance, the values of  $V_g/V_m$  that we observe are consistent with strong stabilizing selection which removes deleterious mutations quickly from the population via natural selection acting directly on the environmentally induced, plastic phenotype.

We found that values of  $V_g/V_m$  in areas of largest plasticity are substantially lower than previously reported data (for example, ref. <sup>54</sup>). Thus, the question arises why mutational variance among clonally related strains is larger than the observed genetic variation among individuals from the outbred population in the dorsal region where defence morphologies are expressed. Our analyses indicate that neither experimental artefacts nor maternal effects are the sole drivers of the observed substantial variation among clonally related strains (Extended Data Fig. 8) and the small values of  $V_g/V_m$  (Fig. 3a,b). Consequently, we speculate that temporal or spatial variation in the strength of selection is a potential factor driving the observed pattern. Population genomic analyses of our natural population indicate that the outbred strains are derived from individuals that recently hatched from sexual ephippia deposited some time in the past, whereas the clonally related strains were present in the population for an extended period of time leading up to the point of collection. If, for instance, the strength of predation varied through time, selection events further in the past may have depleted diversity in the genetically unique clones that result from sexual reproduction (our outbred population), while clonally related strains may have radiated over the last several generations before sampling and reflect more recent population history when the risk of predation was decreased. Alternatively, spatial differences in the ecology of the sampled ponds may have contributed to the observed patterns: a large fraction of the tested, genetically divergent clones originated from one of the two ponds, whereas most of the genetically similar clones were collected from the other pond. However, our analyses of the sampled metapopulation indicate that the two ponds are partly interconnected, allowing for sufficient migration between the two habitats<sup>35</sup>.

Examination of the evolutionary forces acting on environmentally induced traits is important for the interpretation of the evolutionary history of this population and also for assessing its evolutionary potential. While our data show that plasticity is subject to strong stabilizing selection, we also show that there is ample mutational variance for plasticity (Fig. 3). Mutational variance for plasticity could facilitate rapid adaptive evolution following shifts in the predator composition in the aquatic community due to climate change<sup>57,58</sup> or other anthropogenic factors (for example, ref. <sup>59</sup>) and could thus be an important factor facilitating population persistence of *D. pulex* and other organisms, with consequences for ecosystem stability and function<sup>60</sup>.

## Methods

**Study system.** Our data come from a population of *D. pulex* located in the Kilwood Coppice Nature Reserve in the Dorset region of the southern United Kingdom (grid reference: SY 93599 82555). Genotypes used in this study were sampled

from two partly interconnected seasonal ponds with predominantly invertebrate predators during early spring in 2016 and 2017 (Supplementary Table 2). In the laboratory, sampled live individuals were established as isofemale clonal lineages and maintained in artificial hard water (ASTM; ref. <sup>61</sup>) with seaweed extract (marinure; Wilfrid Smith Std) under standard conditions: 15 animals per litre of ASTM were fed three times a week with *Chlorella vulgaris* ( $2 \times 10^5$  cells ml<sup>-1</sup>;  $>1.5$  mg Cl<sup>-1</sup>) and reared under 16:8 h light:dark conditions at 20°C.

**Genotyping. Sequencing.** Full genome sequence data were obtained for the 105 isofemale lines used in this study. For DNA extractions, many adult *Daphnia* were placed into artificial hard water containing antibiotics (streptomycin, tetracycline and ampicillin, 50 mg l<sup>-1</sup> of each) and fed Sephadex G-25 Superfine (cross-linked dextran gel) beads for 48 h to minimize bacterial and algal contamination in downstream sequencing analyses. Five to ten individuals from each clonal lineage were then used for DNA extraction using Beckman-Coulter's Agencourt DNaDvance kit. Individuals were homogenized using metal beads and a bead beater before DNA extraction. RNA was removed using RNase followed by an additional bead clean-up. DNA was quantified using the broad-range Quant-iT dsDNA kit (ThermoFisher Scientific) and an ABI plate reader and normalized to 1 or 2 ng µl<sup>-1</sup> before library construction. Full genome libraries were constructed using a modified down Nextera protocol<sup>62</sup>. Libraries were size selected for fragments ranging from 450 to 550 base pairs (bp) using Blue Pippin and quality checked using BioAnalyzer. Libraries were sequenced at HudsonAlpha Institute for Biotechnology using the Illumina HiSeq 2500 platform.

**Mapping, SNP calling and SNP filtering.** Nextera adaptor sequences were removed using Trimmomatic v0.36 (ref. <sup>63</sup>) and overlapping reads were merged using PEAR v0.9.11 (ref. <sup>64</sup>). Assembled and unassembled reads were separately mapped to a European *D. pulex* reference genome<sup>35</sup> using bwa mem<sup>65</sup>. The entire reference genome was used for mapping but only reads that mapped to *Daphnia* scaffolds, had quality scores  $>20$  and were primary alignments were used for further analysis. PCR duplicates were removed using Picard's MarkDuplicates v.2.20 function<sup>66</sup>. GATK HaplotypeCaller (v4.0; refs. <sup>67,68</sup>) was used to call single-nucleotide polymorphisms (SNPs). We removed SNPs that were within 10 bp of indels. SNPs were then hard filtered using GATK's recommendations for organisms with no reference SNP panel (QD  $< 2$ , FS  $> 60$ , MQ  $< 40$ , MQRankSum  $< -12.5$  and ReadPosRankSum  $< -8$ ). Individual genotype calls with low quality scores (GQ  $< 10$ ) were set as missing data.

**Clonal assignment.** Individual field isolates were assigned to clonal lineages on the basis of patterns of identity by state (IBS). IBS was calculated using the snpgdsIBS function in SNPRelate v1.1.30 (ref. <sup>69</sup>), with a minor allele frequency cutoff of 0.05 and a missing rate of 0.15. We classified individual field isolates as coming from the same clonal lineage if pairwise identity by states was  $>0.965$  (see ref. <sup>35</sup> for more details). We identified 49 genetically unique isofemale lines and one cluster of 56 genetically similar strains, yielding 105 strains that were used for phenotypic analysis. We investigated patterns of relatedness by calculating IBS0 and kinship coefficients using the program KING v.2.2 (ref. <sup>70</sup>). KING was run using the 'kinship' command with the input data filtered to include SNPs with a minor allele frequency cutoff of 0.05.

**Phenotyping. Experimental exposures.** Phenotypic data were collected for the described 105 isofemale lines (Supplementary Table 2). To establish predation risk conditions, we generated predator cues from frozen midge larvae (*Chaoborus* spp.) following established protocols<sup>71</sup>. Homogenized midge larvae extracts were filtered, followed by solid-phase extraction using a C<sub>18</sub> column (Agilent) to recover the active compounds that generate strong morphological responses in *D. pulex*. For experimental exposures, animals were kept under standard conditions for three generations. Subsequently, at least two gravid *Daphnia*, carrying embryos in E<sub>3</sub> stage (~18 h before parturition; sensu ref. <sup>72</sup>), were placed in individual jars containing 50 ml of hard artificial pond water<sup>61</sup>, algae ( $2 \times 10^5$  cells ml<sup>-1</sup> of *C. vulgaris*), liquid seaweed extract and 0 or 0.5 µl ml<sup>-1</sup> of *Chaoborus* predator cue concentrate. After parturition, two neonates were randomly selected from each of the two mothers per treatment and placed individually in 50 ml glass vials containing the same medium as their maternal environment. For 3–4 consecutive days, each animal was photographed daily (Leica S8AP0 microscope; Leica EC4 camera) while placing each animal briefly onto an object slide and subsequently transferred to a new glass vial containing fresh media and predator cues. Due to the large amount of experimental exposures, phenotypic assessments were carried in a split-block experimental design across 20 experimental batches in total, with experimental exposure jars randomized across the rearing set-up. On average, eight strains (random choice of four clonal related and four genetically unique strains) were phenotyped concurrently per batch, with exposures relatively evenly split between treatment groups and clonal and outbred individuals.

**High-throughput image analysis.** We assessed phenotypic changes using an automated image analysis pipeline hereafter referred to as DAPCHA (Supplementary Methods). To validate accurate performance of DAPCHA, all images were manually checked and, if required, landmarks manually curated.

We recorded manual estimates of units of microstage meter (~100 randomly chosen images) via two separate runs of estimation and animal lengths and morphological induction (>700 randomly chosen images) via three independent observers using ImageJ software (v.1.51a; refs. <sup>73,74</sup>). We manually measured animal length from the tip of the head to the base of the tail. Morphological induction, based on the presence of a pedestal, was manually scored using a previously defined scoring system<sup>29,33</sup>. Developed spikes in the nuchal area, referred to as neckteeth, were counted individually. To account for size differences among clonal lineages and exclude size-dependent estimates in our analyses, we normalized dorsal height by animal length for all downstream analyses.

**Instar assignment.** Animals were retroactively assigned to distinct developmental stages (first and second instar) by fitting a mixture model on animal dorsal area and animal length, using the Mclust package (v.5.4.6) for R (ref. <sup>75</sup>).

**Analysis of variance.** To assess the contribution of genotype, treatment and their interaction on dorsal height, we fit a linear model (dorsal height ~ genotype \* treatment + batch), followed by type II sums of squares implemented by the Anova() function in the car package for R (ref. <sup>76</sup>) for significance testing and estimation of effect sizes using the effectsize package (v.0.4.4) for R (ref. <sup>77</sup>).

**Magnitude and position of induced defence.** To estimate how predation risk altered the magnitude and position of the morphological defence structures, we applied a phenotypic trajectory analysis<sup>39</sup> to the multivariate data matrix of dorsal height at each *i*th position along the dorsal edge using the geomorph package (v.3.3.1) for R (refs. <sup>40,78,79</sup>). We fit a model where the response variable is the multivariate dorsal height  $\times$  position matrix among genotypes versus treatment (control – predation). We estimated the overall impact of predation risk using 1,000 permutations via the procD.lm() function. This was followed by assessment of the direction and magnitude statistics via the trajectory.analysis() function. Visualization of the morphology and details about the shift in height and position of maximal induction were made with the plotRefToTarget() function.

To assess modularity and identify whether the region where the morphological defence is induced is correlated (or not) with the rest of the body, we applied the modularity.test() function in the geomorph package (v.3.3.1) for R (refs. <sup>40,78,79</sup>). This function quantifies the degree of modularity in two or more suggested modules of shape variables (here using dorsal positions 10 to 600) and compares this to what is expected under the null hypothesis of random assignment of variables to partitions (neither modular nor integrated structure). The extent of modularity is described by CR which depicts the ratio of the overall covariation between modules relative to the overall covariation within modules. A statistically significant modular signal is found when the observed CR coefficient is small relative to this distribution (ref. <sup>40</sup>). Such a result implies that there is greater independence among modules than is expected under the null hypothesis of random association of variables. We specifically constructed 13 module configurations that varied in both the number of modules and the location of the module breakpoints (Extended Data Fig. 5) and tested for the presence of modularity between areas of largest plasticity (head region) and the remaining dorsal areas along the carapace. To identify the strongest statistical support for modular structures, we applied the R function compare.CR() in the geomorph package (v.3.3.1) for R (ref. <sup>41</sup>) and corrected obtained *P* values for multiple testing using the p.adjust() function with Bonferroni correction.

**Twin analysis.** To assess how much offspring resemble one another when released from (1) the same mother and the same clutch, (2) the same strain but different mother, (3) randomly drawn strains from the clonal assemblage of genetically similar strains and (4) randomly drawn individuals from each experimental batch, we performed a correlation analysis for two key phenotypic traits, animal length and maximal dorsal height, using the R package robcor (v.0.1–6) (ref. <sup>80</sup>). To estimate correlation coefficients for randomly drawn clone pairs from among genetically similar strains or batches, we performed 100 bootstraps. To contrast observed correlation coefficients to a NULL distribution, we permuted phenotypic data ( $n = 1,000$ ) and tested for differences between observed and permuted data using a non-parametric Wilcoxon rank sum test.

**Heritability estimation.** We first estimated broad-sense heritability of phenotypic traits for the genetically unique strains and the clonally related strains within environments using a model of:

$$\text{dorsal height} \sim 1, \text{random} = \sim 1|\text{clone} + \sim 1|\text{batch}.$$

The models were estimated using MCMCglmm (v.2.29)<sup>81</sup> in a Bayesian framework with priors set as default, 65,000 MCMC iterations, a thinning interval of 50 and a burn-in of 15,000, producing 1,300 posterior estimates. We then used the posterior distribution associated with the clone term from each of these models to estimate the  $V_g/V_m$  ratio in each environment, where  $V_g$  is the clone term variance estimate for the genetically unique strain model and  $V_m$  the clone term variance estimate for the clonally related strain model. To generate our  $V_g/V_m$  inference, with a credible interval, we applied the formula  $\log_{10}(V_g) - \log_{10}(V_m)$ .

This produced a posterior mean and credible interval for  $V_g/V_m$ . All models were checked for autocorrelation in the chains.

We next estimated narrow-sense heritability of phenotypic traits in the genetically divergent clones using GCTA (v.1.93.2)<sup>82</sup>. We calculated a genetic relatedness matrix from genome-wide SNPs (MAF = 0.05) with the --make-grm flag in GCTA. For heritability estimate calculations, we used the flags --reml, --reml-alg 1, accounting for batch as covariate. To determine heritability estimates for random data (NULL distribution), we permuted genome identifiers before calculating genetic relatedness matrices.

**Statistical analysis and plotting.** All analyses were performed using R (v.3.5)<sup>83</sup>. The following packages were used for general analysis and plotting: ggplot2 (v.3.3.3)<sup>84</sup>, cowplot (v.1.1.0)<sup>85</sup>, data.table (v.1.14.0)<sup>86</sup>, foreach (v.1.5.1)<sup>87</sup>, doMC (v.1.3.7)<sup>88</sup>, ggbbeeswarm (v.0.6.0)<sup>89</sup> and viridis (v.0.5.1)<sup>90</sup>.

**Reporting summary.** Further information on research design is available in the Nature Research Reporting Summary linked to this article.

## Data availability

All raw images and processed data used to generate figures are deposited in Zenodo (<https://doi.org/10.5281/zenodo.4738526>). All sequencing reads are available from the Sequence Read Archive (PRJNA725506).

## Code availability

All scripts and code used for data analysis and plotting are available at <https://github.com/beckerdoerthe/SelectionPlasticity>. DAPCHA is available at [https://github.com/beckerdoerthe/Dapcha\\_v1](https://github.com/beckerdoerthe/Dapcha_v1).

Received: 12 July 2021; Accepted: 20 June 2022;

Published online: 18 August 2022

## References

- Scheiner, S. M. Genetics and evolution of phenotypic plasticity. *Annu. Rev. Ecol. Syst.* **24**, 35–68 (1993).
- Via, S. et al. Adaptive phenotypic plasticity: consensus and controversy. *Trends Ecol. Evol.* **10**, 212–217 (1995).
- Ghalambor, C. K. et al. Adaptive versus non-adaptive phenotypic plasticity and the potential for contemporary adaptation in new environments. *Funct. Ecol.* **21**, 394–407 (2007).
- King, J. G. & Hadfield, J. D. The evolution of phenotypic plasticity when environments fluctuate in time and space. *Evol. Lett.* **3**, 15–27 (2019).
- Newman, R. A. Genetic variation for phenotypic plasticity in the larval life history of spadefoot toads (*Scaphiopus couchii*). *Evolution* **48**, 1773–1785 (1994).
- Nussey, D. H. et al. Selection on heritable phenotypic plasticity in a wild bird population. *Science* **310**, 304–306 (2005).
- Scheiner, S. Selection experiments and the study of phenotypic plasticity 1. *J. Evol. Biol.* **15**, 889–898 (2002).
- Ghalambor, C. K. et al. Non-adaptive plasticity potentiates rapid adaptive evolution of gene expression in nature. *Nature* **525**, 372–375 (2015).
- Reger, J. et al. Predation drives local adaptation of phenotypic plasticity. *Nat. Ecol. Evol.* **2**, 100–107 (2018).
- Sommer, R. J. Phenotypic plasticity: from theory and genetics to current and future challenges. *Genetics* **215**, 1–13 (2020).
- Brakefield, P. M. & Reitsma, N. Phenotypic plasticity, seasonal climate and the population biology of *Bicyclus* butterflies (Satyridae) in Malawi. *Ecol. Entomol.* **16**, 291–303 (1991).
- Rountree, D. & Nijhout, H. Hormonal control of a seasonal polyphenism in *Precis coenia* (Lepidoptera: Nymphalidae). *J. Insect Physiol.* **41**, 987–992 (1995).
- Scheiner, S. M. & Holt, R. D. The genetics of phenotypic plasticity. X. Variation versus uncertainty. *Ecol. Evol.* **2**, 751–767 (2012).
- Bonamour, S. et al. Phenotypic plasticity in response to climate change: the importance of cue variation. *Philos. Trans. R. Soc. B* **374**, 20180178 (2019).
- Fox, R. J., Donelson, J. M., Schunter, C., Ravasi, T. & Gaitán-Espitia, J. D. Beyond buying time: the role of plasticity in phenotypic adaptation to rapid environmental change. *Philos. Trans. R. Soc. B* <https://doi.org/10.1098/rstb.2018.0174> (2019).
- Auld, J. R., Agrawal, A. A. & Relyea, R. A. Re-evaluating the costs and limits of adaptive phenotypic plasticity. *Proc. R. Soc. B* **277**, 503–511 (2010).
- Murren, C. J. et al. Constraints on the evolution of phenotypic plasticity: limits and costs of phenotype and plasticity. *Heredity* **115**, 293–301 (2015).
- Yampolsky, L. Y., Schaer, T. M. & Ebert, D. Adaptive phenotypic plasticity and local adaptation for temperature tolerance in freshwater zooplankton. *Proc. R. Soc. B* **281**, 20132744 (2014).
- Schmid, M. & Guillaume, F. The role of phenotypic plasticity on population differentiation. *Heredity* **119**, 214–225 (2017).

20. Charlesworth, B., Lande, R. & Slatkin, M. A neo-Darwinian commentary on macroevolution. *Evolution* **36**, 474–498 (1982).
21. Lynch, M. The rate of morphological evolution in mammals from the standpoint of the neutral expectation. *Am. Nat.* **136**, 727–741 (1990).
22. Kingsolver, J. G. & Pfennig, D. W. Patterns and power of phenotypic selection in nature. *Bioscience* **57**, 561–572 (2007).
23. West-Eberhard, M. J. Developmental plasticity and the origin of species differences. *Proc. Natl Acad. Sci. USA* **102**, 6543–6549 (2005).
24. Turelli, M. & Barton, N. Polygenic variation maintained by balancing selection: pleiotropy, sex-dependent allelic effects and  $G \times E$  interactions. *Genetics* **166**, 1053–1079 (2004).
25. Charlesworth, B. Causes of natural variation in fitness: evidence from studies of *Drosophila* populations. *Proc. Natl Acad. Sci. USA* **112**, 1662–1669 (2015).
26. Noble, D. W., Radersma, R. & Uller, T. Plastic responses to novel environments are biased towards phenotype dimensions with high additive genetic variation. *Proc. Natl Acad. Sci. USA* **116**, 13452–13461 (2019).
27. Draghi, J. A. & Whitlock, M. C. Phenotypic plasticity facilitates mutational variance, genetic variance, and evolvability along the major axis of environmental variation. *Evolution* **66**, 2891–2902 (2012).
28. Houle, D. How should we explain variation in the genetic variance of traits? *Genetica* **102**, 241–253 (1998).
29. Tollrian, R. Predator-induced morphological defenses: costs, life history shifts, and maternal effects in *Daphnia pulex*. *Ecology* **76**, 1691–1705 (1995).
30. Agrawal, A. A., Laforsch, C. & Tollrian, R. Transgenerational induction of defences in animals and plants. *Nature* **401**, 60–63 (1999).
31. Tollrian, R. Neckteeth formation in *Daphnia pulex* as an example of continuous phenotypic plasticity: morphological effects of *Chaoborus* kairomone concentration and their quantification. *J. Plankton Res.* **15**, 1309–1318 (1993).
32. Dennis, S. et al. Phenotypic convergence along a gradient of predation risk. *Proc. R. Soc. B* **278**, 1687–1696 (2011).
33. Hammill, E. & Beckerman, A. P. Reciprocity in predator-prey interactions: exposure to defended prey and predation risk affects intermediate predator life history and morphology. *Oecologia* **163**, 193–202 (2010).
34. Hammill, E., Rogers, A. & Beckerman, A. P. Costs, benefits and the evolution of inducible defences: a case study with *Daphnia pulex*. *J. Evol. Biol.* **21**, 705–715 (2008).
35. Barnard-Kubow, K. et al. Polygenic variation in sexual investment across an ephemerality gradient in *Daphnia pulex*. *Mol. Bio. Evol.* **39**, msac121 (2022).
36. Deng, H.-W. & Lynch, M. Inbreeding depression and inferred deleterious-mutation parameters in *Daphnia*. *Genetics* **147**, 147–155 (1997).
37. Seyfert, A. L. et al. The rate and spectrum of microsatellite mutation in *Caenorhabditis elegans* and *Daphnia pulex*. *Genetics* **178**, 2113–2121 (2008).
38. Xu, S. et al. High mutation rates in the mitochondrial genomes of *Daphnia pulex*. *Mol. Biol. Evol.* **29**, 763–769 (2012).
39. Collyer, M. L. & Adams, D. C. Phenotypic trajectory analysis: comparison of shape change patterns in evolution and ecology. *Hystrix* **24**, 75 (2013).
40. Adams, D.C., Collyer, M., Kaliontzopoulou, A. & Sherratt, E. et al. Geomorph: software for geometric morphometric analyses (University of New England, 2016); <https://hdl.handle.net/1959.11/21330>
41. Adams, D. C. & Collyer, M. L. Comparing the strength of modular signal, and evaluating alternative modular hypotheses, using covariance ratio effect sizes with morphometric data. *Evolution* **73**, 2352–2367 (2019).
42. Richards, C. L., Bossdorf, O. & Pigliucci, M. What role does heritable epigenetic variation play in phenotypic evolution? *BioScience* **60**, 232–237 (2010).
43. Latta, L. C. IV et al. The phenotypic effects of spontaneous mutations in different environments. *Am. Nat.* **185**, 243–252 (2015).
44. Lind, M. I. et al. The alignment between phenotypic plasticity, the major axis of genetic variation and the response to selection. *Proc. R. Soc. B* **282**, 20151651 (2015).
45. Laforsch, C. & Tollrian, R. Inducible defenses in multipredator environments: cyclomorphosis in *Daphnia cucullata*. *Ecology* **85**, 2302–2311 (2004).
46. Weiss, L. C., Leimann, J. & Tollrian, R. Predator-induced defences in *Daphnia longicephala*: location of kairomone receptors and timeline of sensitive phases to trait formation. *J. Exp. Biol.* **218**, 2918–2926 (2015).
47. Tollrian, R. & Harvell, C.D. *The Ecology and Evolution of Inducible Defenses* (Princeton Univ. Press, 1999).
48. Lande, R. Adaptation to an extraordinary environment by evolution of phenotypic plasticity and genetic assimilation. *J. Evol. Biol.* **22**, 1435–1446 (2009).
49. Via, S. & Lande, R. Genotype-environment interaction and the evolution of phenotypic plasticity. *Evolution* **39**, 505–522 (1985).
50. Kvist, J. et al. Temperature treatments during larval development reveal extensive heritable and plastic variation in gene expression and life history traits. *Mol. Ecol.* **22**, 602–619 (2013).
51. Siepielski, A. M. et al. Differences in the temporal dynamics of phenotypic selection among fitness components in the wild. *Proc. R. Soc. B* **278**, 1572–1580 (2011).
52. Muschick, M. et al. Adaptive phenotypic plasticity in the Midas cichlid fish pharyngeal jaw and its relevance in adaptive radiation. *BMC Evol. Biol.* **11**, 116 (2011).
53. Salzburger, W. Understanding explosive diversification through cichlid fish genomics. *Nat. Rev. Genet.* **19**, 705–717 (2018).
54. Halligan, D. L. & Keightley, P. D. Spontaneous mutation accumulation studies in evolutionary genetics. *Annu. Rev. Ecol. Evol. Syst.* **40**, 151–172 (2009).
55. Houle, D., Morikawa, B. & Lynch, M. Comparing mutational variabilities. *Genetics* **143**, 1467–1483 (1996).
56. Eberle, S. et al. Hierarchical assessment of mutation properties in *Daphnia magna*. *G3 Genes Genomes Genetics* **8**, 3481–3487 (2018).
57. Stenseth, N. C. et al. Ecological effects of climate fluctuations. *Science* **297**, 1292–1296 (2002).
58. Burgmer, T., Hillebrand, H. & Pfenniger, M. Effects of climate-driven temperature changes on the diversity of freshwater macroinvertebrates. *Oecologia* **151**, 93–103 (2007).
59. Yan, N. D. et al. Long-term trends in zooplankton of Dorset, Ontario, lakes: the probable interactive effects of changes in pH, total phosphorus, dissolved organic carbon, and predators. *Can. J. Fish. Aquat. Sci.* **65**, 862–877 (2008).
60. Reed, T. E., Schindler, D. E. & Waples, R. S. Interacting effects of phenotypic plasticity and evolution on population persistence in a changing climate. *Conserv. Biol.* **25**, 56–63 (2011).
61. ASTM, *Standard Guide for Conducting Acute Toxicity Tests with Fishes, Macroinvertebrates, and Amphibians* (American Society for Testing and Materials, 1988).
62. Baym, M. et al. Inexpensive multiplexed library preparation for megabase-sized genomes. *PLoS ONE* **10**, e0128036 (2015).
63. Bolger, A. M., Lohse, M. & Usadel, B. Trimmomatic: a flexible trimmer for Illumina sequence data. *Bioinformatics* **30**, 2114–2120 (2014).
64. Zhang, J. et al. PEAR: a fast and accurate Illumina Paired-End reAd merger. *Bioinformatics* **30**, 614–620 (2014).
65. Li, H. Aligning sequence reads, clone sequences and assembly contigs with BWA-MEM. Preprint at <https://arxiv.org/abs/1303.3997> (2013).
66. MarkDuplicates v2.20 (Broad Institute, 2019); <http://broadinstitute.github.io/picard>
67. McKenna, A. et al. The Genome Analysis Toolkit: a MapReduce framework for analyzing next-generation DNA sequencing data. *Genome Res.* **20**, 1297–1303 (2010).
68. Poplin, R. et al. Scaling accurate genetic variant discovery to tens of thousands of samples. Preprint at *bioRxiv* <https://doi.org/10.1101/201178> (2018).
69. Zheng, X. et al. A high-performance computing toolset for relatedness and principal component analysis of SNP data. *Bioinformatics* **28**, 3326–3328 (2012).
70. Manichaikul, A. et al. Robust relationship inference in genome-wide association studies. *Bioinformatics* **26**, 2867–2873 (2010).
71. Beckerman, A. P., Rodgers, G. M. & Dennis, S. R. The reaction norm of size and age at maturity under multiple predator risk. *J. Anim. Ecol.* **79**, 1069–1076 (2010).
72. Naraki, Y., Hirata, C. & Tochinai, S. Identification of the precise kairomone-sensitive period and histological characterization of necktooth formation in predator-induced polyphenism in *Daphnia pulex*. *Zool. Sci.* **30**, 619–625 (2013).
73. Schneider, C. A., Rasband, W. S. & Eliceiri, K. W. NIH Image to ImageJ: 25 years of image analysis. *Nat. Methods* **9**, 671–675 (2012).
74. Schindelin, J. et al. Fiji: an open-source platform for biological-image analysis. *Nat. Methods* **9**, 676–682 (2012).
75. Scrucca, L. et al. mclust 5: clustering, classification and density estimation using Gaussian finite mixture models. *R J.* **8**, 289 (2016).
76. Fox, J. & Weisberg, S. *An R Companion to Applied Regression* (Sage, 2018).
77. Ben-Shachar, M. S., Lüdecke, D. & Makowski, D. effectsize: estimation of effect size indices and standardized parameters. *J. Open Source Softw.* **5**, 2815 (2020).
78. Collyer, M. L. & Adams, D. C. RRPP: an r package for fitting linear models to high-dimensional data using residual randomization. *Methods Ecol. Evol.* **9**, 1772–1779 (2018).
79. Collyer, M., Adams, D. & Collyer, M.M. RRPP: linear model evaluation with randomized residuals in a permutation procedure. R package version 1.3 <https://CRAN.R-project.org/package=RRPP> (2021).
80. Smirnov, P. robcor: Robust correlations. R package version 0.1-6.1 <https://CRAN.R-project.org/package=ropcor> (2014).
81. Hadfield, J. D. MCMC methods for multi-response generalized linear mixed models: the MCMCglmm R package. *J. Stat. Softw.* **33**, 1–22 (2010).
82. Yang, J. et al. GCTA: a tool for genome-wide complex trait analysis. *Am. J. Hum. Genet.* **88**, 76–82 (2011).
83. R Core Team. *R: A Language and Environment for Statistical Computing* (R Foundation for Statistical Computing, 2017).
84. Villanueva, R., Chen, Z. & Wickham, H. *ggplot2: Elegant Graphics for Data Analysis Using the Grammar of Graphics* (Springer-Verlag, 2016).

85. Wilke, C. cowplot: Streamlined plot theme and plot annotations for 'ggplot2'. R package version 0.9. 2 <https://CRAN.R-project.org/package=cowplot> (2020).
86. Dowle, M. et al. data.table: Extension of 'data.frame'. R package version 1.14.0 <https://CRAN.R-project.org/package=data.table> (2021).
87. Daniel, M. foreach: Provides foreach looping construct. R package version 1.5.1 <https://CRAN.R-project.org/package=foreach> (2020).
88. Weston, S. doMC: Foreach parallel adaptor for 'parallel'. R package version 1.3.7 <https://CRAN.R-project.org/package=doMC> (2020).
89. Clarke, E. & Sherrill-Mix, S. Ggbeeswarm: Categorical scatter (violin point) plots. R package version 0.6. 0 <https://CRAN.R-project.org> (2017).
90. Garnier, S. et al. viridis: Default color maps from 'matplotlib'. R package version 0.5.1 (2018).

## Acknowledgements

A.O.B. was supported by the National Institutes of Health (R35 GM119686) and by start-up funds provided by the University of Virginia. D.B. and A.P.B. were supported by the European Union's Horizon 2020 research and innovation programme under the Marie Skłodowska-Curie grant agreement no. 841419. The authors acknowledge Research Computing at The University of Virginia for providing computational resources and technical support that have contributed to the results reported within this publication (<https://rc.virginia.edu>). We would also like to thank the Dorset Wildlife Trust for granting access to the field site.

## Author contributions

D.B., A.O.B. and A.P.B. were responsible for conceptualization. D.B. and A.O.B. undertook data curation, formal analysis, methodology, resources, software and

visualization and wrote the original draft of the manuscript. A.O.B. obtained funding and was responsible for project administration and supervision. D.B., K.B.-K., R.P., A.E., E.V. and A.O.B. undertook the investigations. All authors were involved in reviewing and editing the manuscript.

## Competing interests

The authors declare no competing interests.

## Additional information

**Extended data** is available for this paper at <https://doi.org/10.1038/s41559-022-01837-5>.

**Supplementary information** The online version contains supplementary material available at <https://doi.org/10.1038/s41559-022-01837-5>.

**Correspondence and requests for materials** should be addressed to Dörthe Becker or Alan O. Bergland.

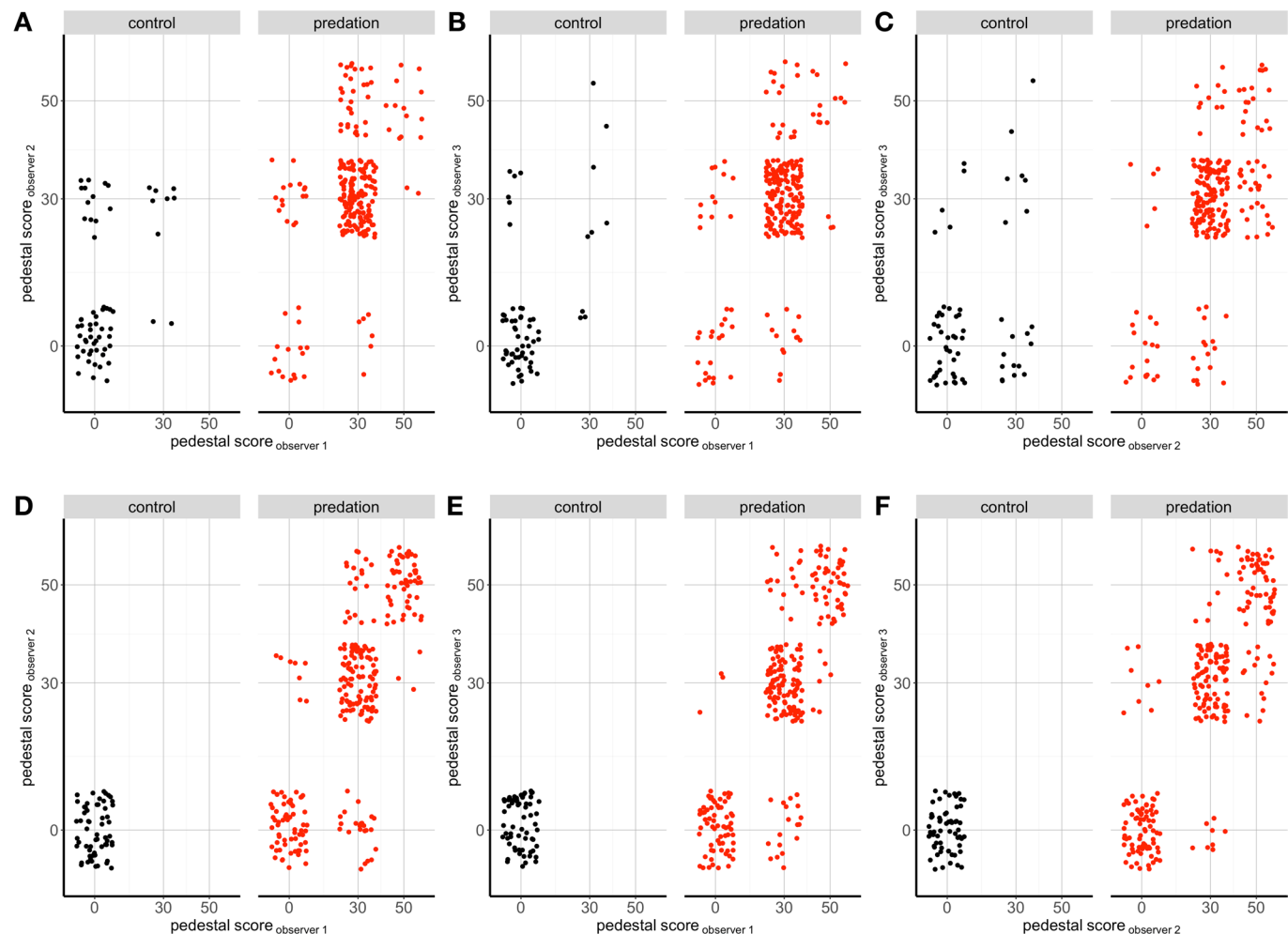
**Peer review information** *Nature Ecology & Evolution* thanks Nicholas Levis, Katja Rasanen and Alison Scoville for their contribution to the peer review of this work.

**Reprints and permissions information** is available at [www.nature.com/reprints](http://www.nature.com/reprints).

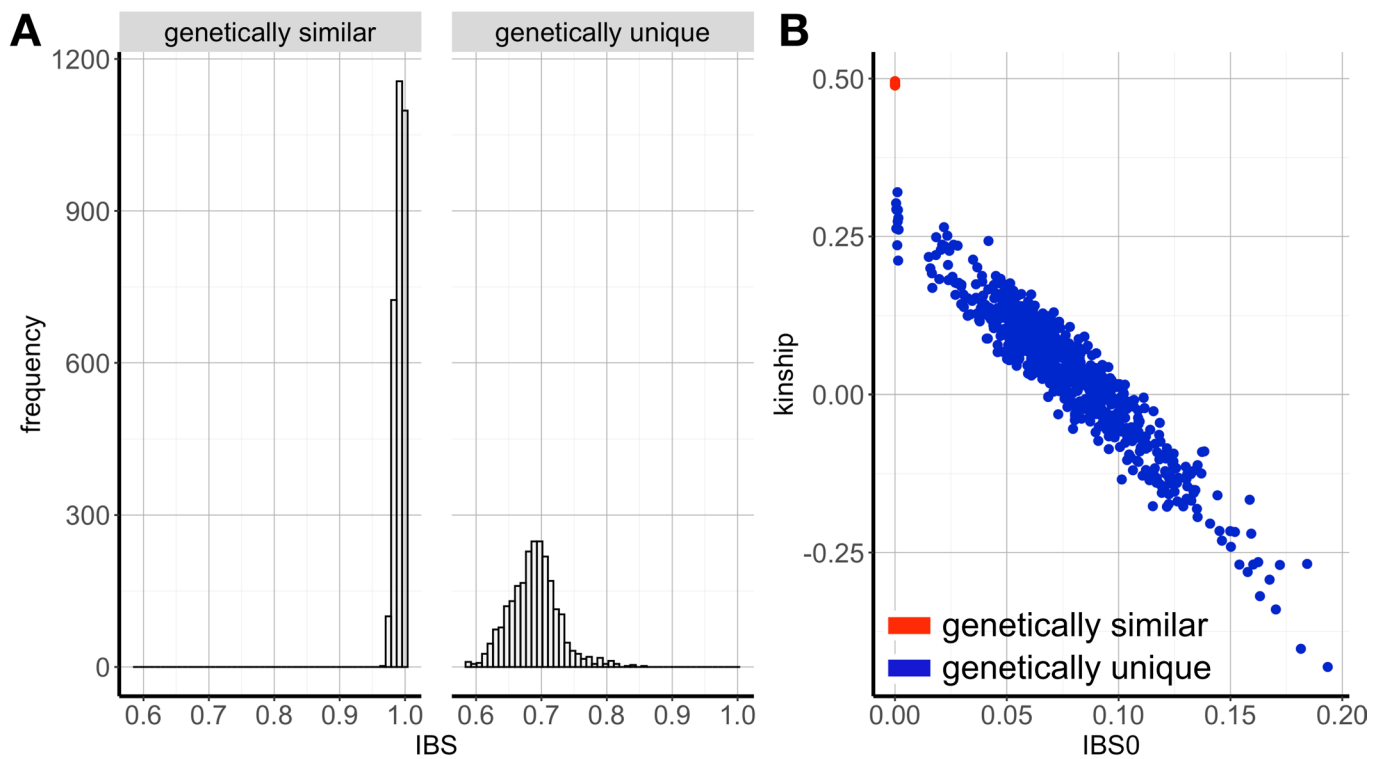
**Publisher's note** Springer Nature remains neutral with regard to jurisdictional claims in published maps and institutional affiliations.

Springer Nature or its licensor holds exclusive rights to this article under a publishing agreement with the author(s) or other rightsholder(s); author self-archiving of the accepted manuscript version of this article is solely governed by the terms of such publishing agreement and applicable law.

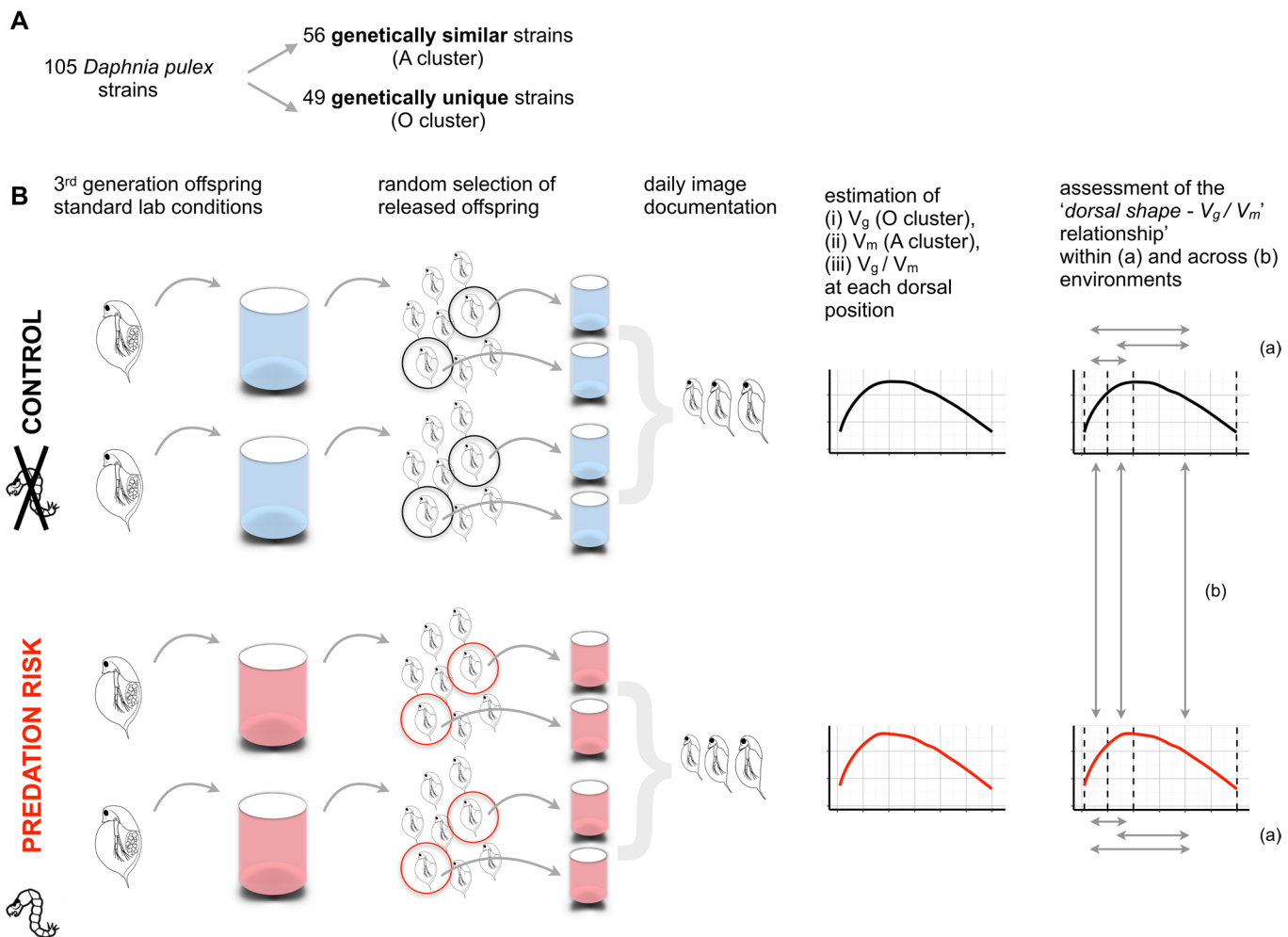
© The Author(s), under exclusive licence to Springer Nature Limited 2022



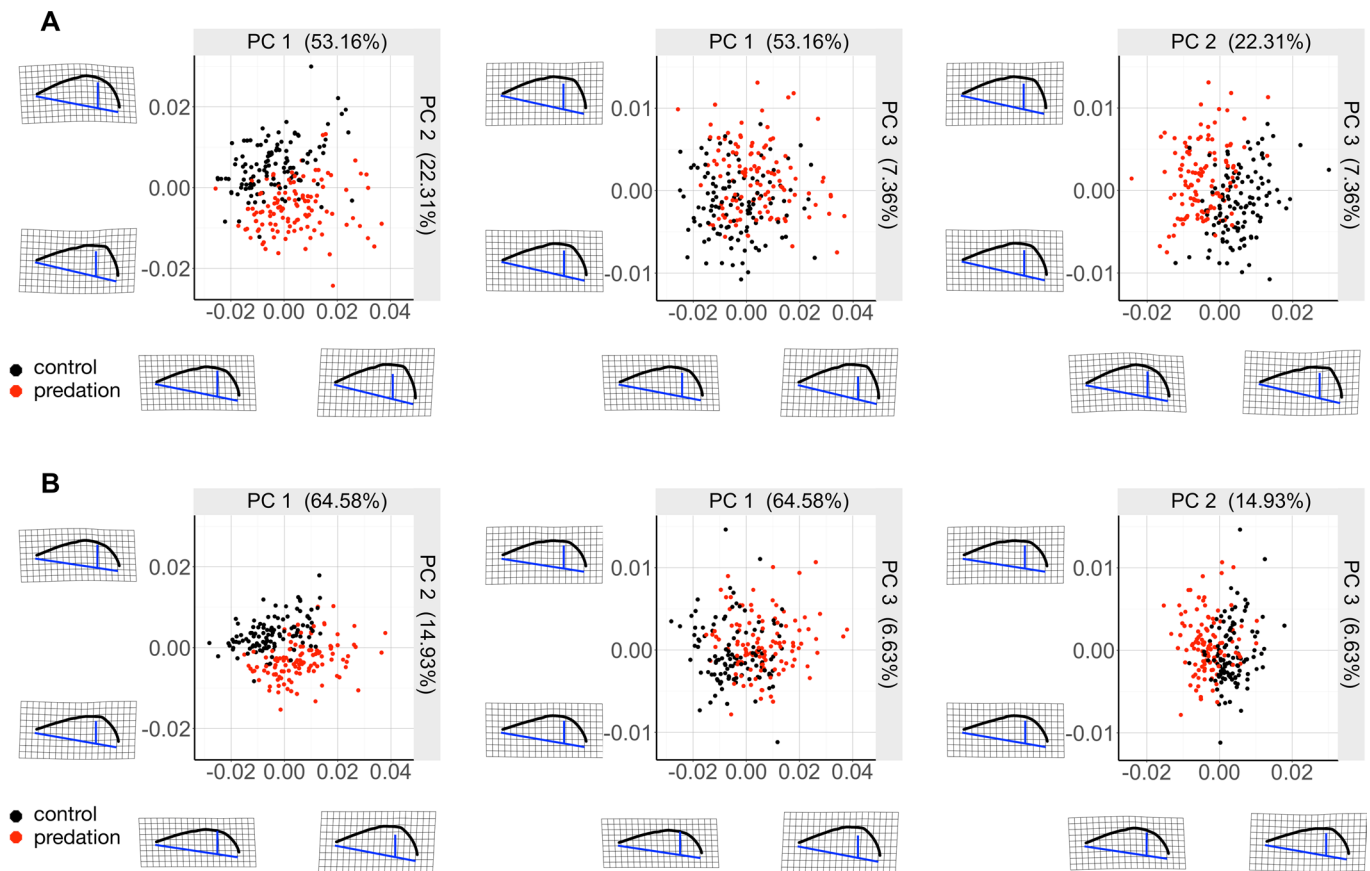
**Extended Data Fig. 1 | Inconsistency in manual assessments of defence morphologies.** Jitter plot contrasting manual estimates of pedestal scores in first (A-C) and second (D-F) instar animals across three independent observers indicates inconsistent manual assessment: while the majority of estimates overlap between the three observers, manual assessments of the pedestal scores differ between observers, particularly under predation conditions.



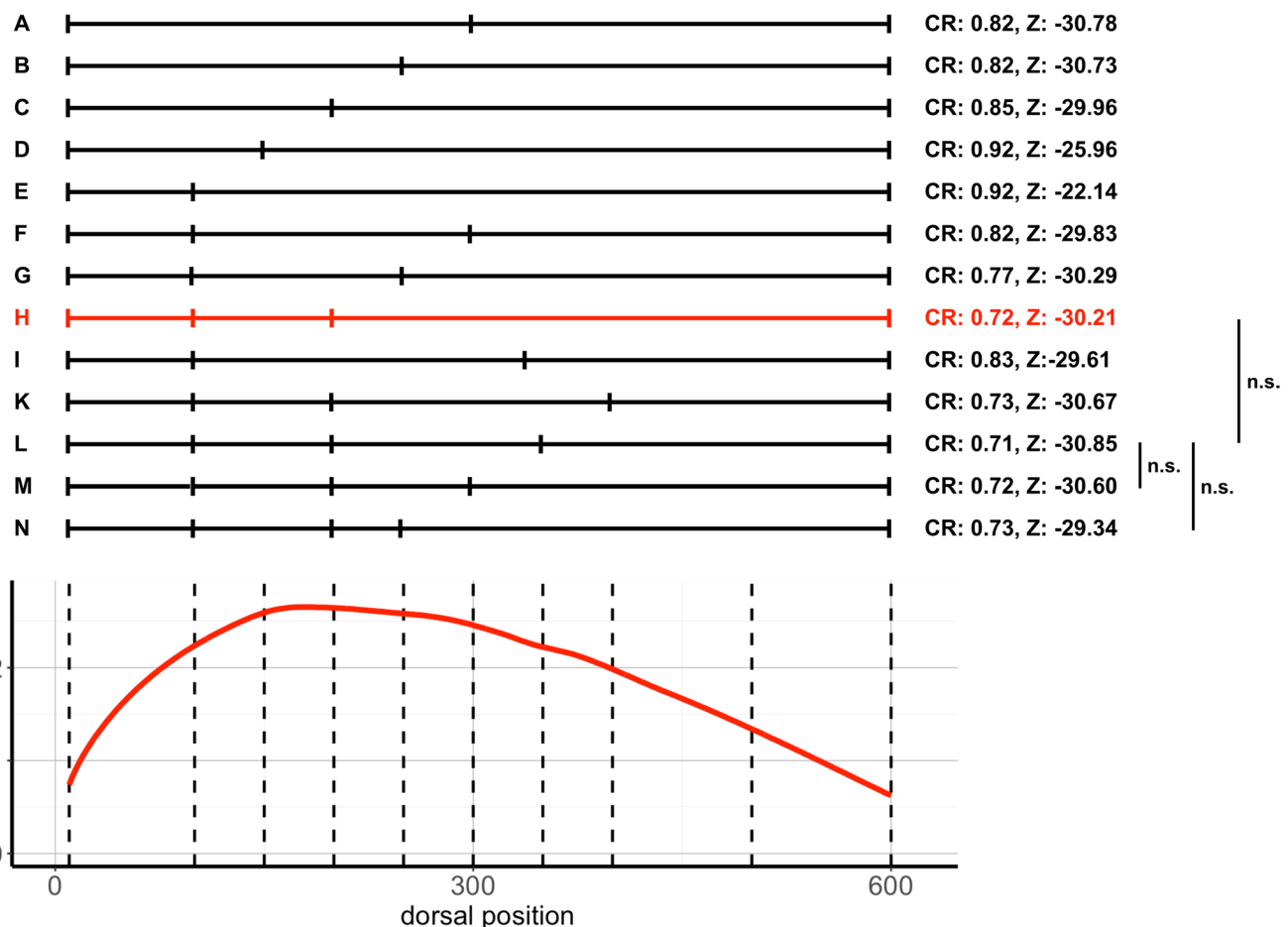
**Extended Data Fig. 2 | Genetic diversity among genetically similar and genetically unique strains.** (A) Distribution of pairwise IBS values between all genetically similar (left) and genetically unique (right) strains. (B) Relationship between IBS0 and kinship as calculated in the program King for pairwise combinations of individuals genotyped from the sampled population. Red and blue circles depict genetically similar and genetically unique strains, respectively. Note that in (B) all comparisons between clonally related strains (red points) are stacked on top of each other.

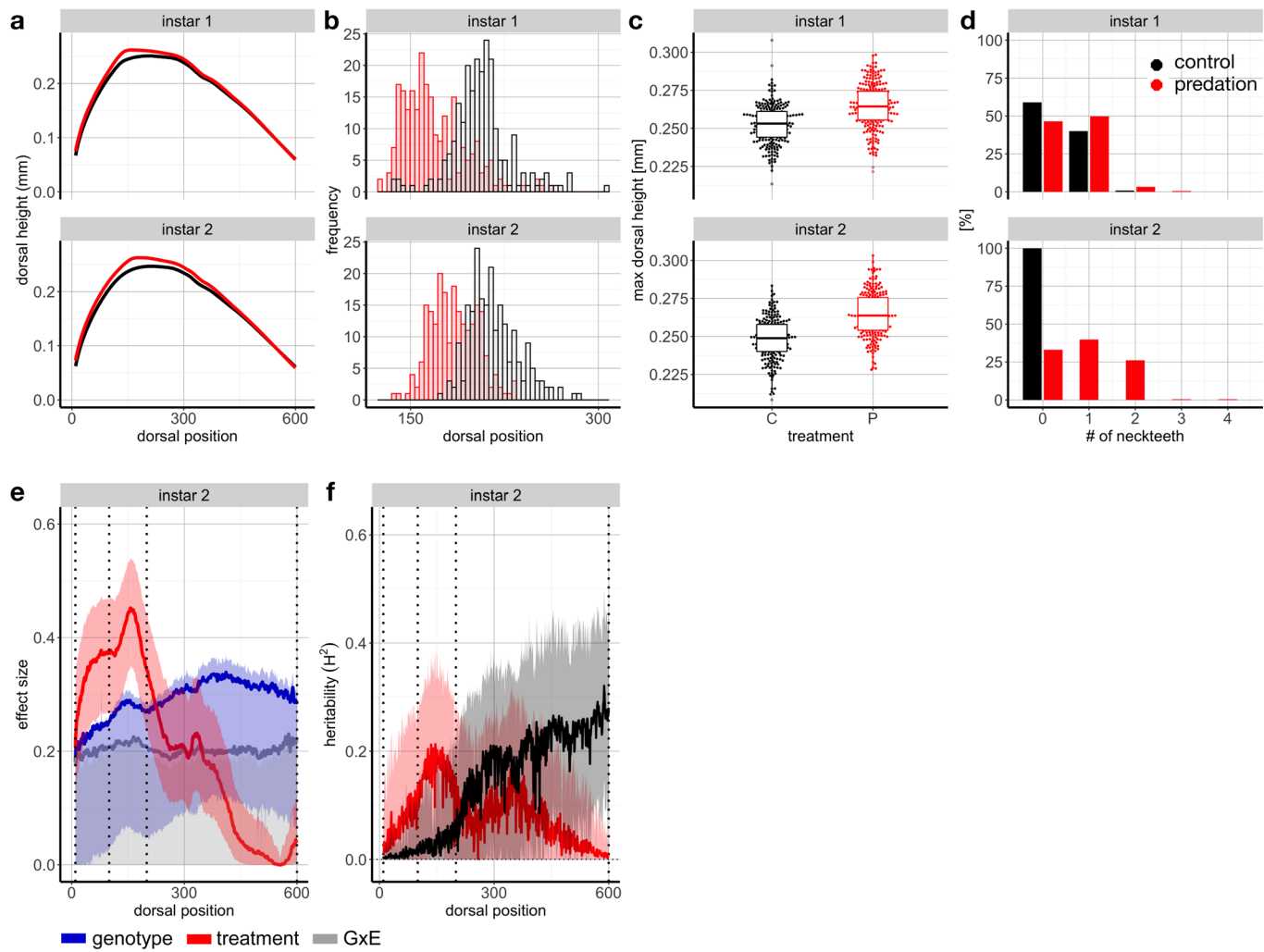


**Extended Data Fig. 3 | Experimental design.** (A) Full genome sequence analyses from 105 isofemale lines identified 49 genetically unique strains and one cluster of 56 genetically similar strains. (B) Phenotypic data were collected for these 105 isofemale lines: For experimental exposures, two mature *Daphnia pulex* carrying embryos in E<sub>3</sub> stage (~18 hours before parturition; sensu<sup>72</sup>) were placed in individual jars containing medium with (bottom panel) and without (top panel) predator cue. After parturition, two neonates were randomly selected from each of the two mothers and placed in individual vials containing the same medium as their maternal environment. Subsequently, animals were monitored for 3–4 consecutive days, with daily photographs taken. Using an automated image analysis pipeline (DAPCHA, see Materials and methods and Suppl. Methods), phenotypic responses to control and predation conditions were assessed (see section ‘Robust and accurate phenotyping’, Fig. 1, Fig. 2a–c, Extended Data Fig. 6a–d). Next, heritability estimates for the observed within generation phenotypic response at each dorsal position were investigated for both genetically similar and genetically unique strains in the absence and presence of predator cue. These data allowed to contrast levels of standing genetic variation ( $V_g$ ) with mutational variation ( $V_m$ ) across the dorsal region. Comparing the patterns of the ‘dorsal region –  $V_g/V_m$  relationship’ within and between treatments ultimately provided evidence of differential selection across the phenotypic trait (see sections ‘Evidence for stabilizing selection in an outbred sample’ and ‘Mutational variation and further evidence of stabilizing selection’; Fig. 2e–h, Fig. 3, Extended Data Fig. 6e, f).

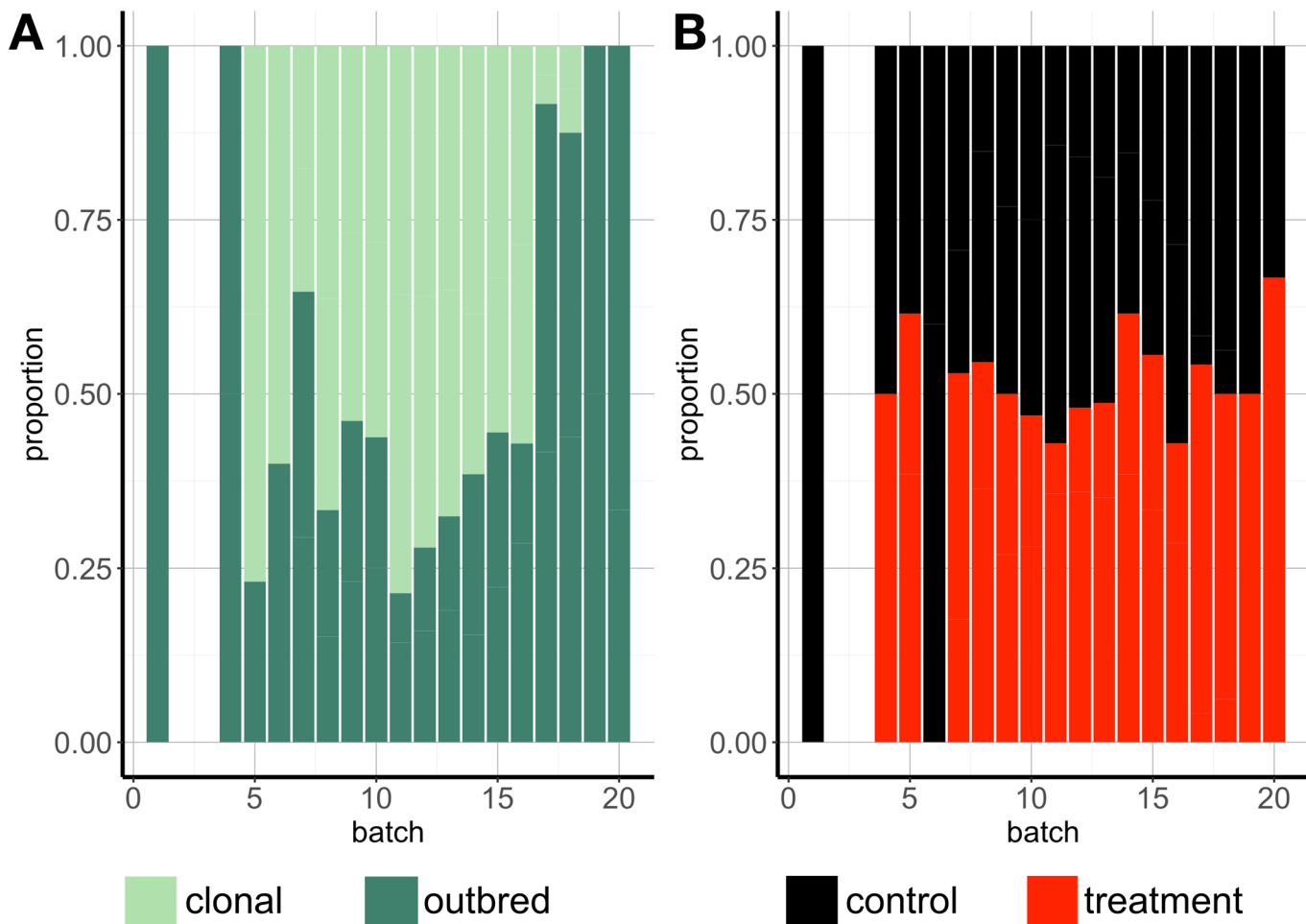


**Extended Data Fig. 4 | Chaoborus induced shape variation in *D. pulex*.** Visualization of the first three main axes of dorsal shape variation in first (A) and second instar (B) *Daphnia* using principal component (PC) analysis of procrustes data. Colours indicate treatment conditions (control: black points, predation: red points). Warp-shape diagrams highlight distinctive patterns of shape variations along the principal components: PC1 represents shape differences in dorsal height, while PC2 and PC3 characterize the development of predator-induced defence morphologies and shifts in their dorsal position, respectively.

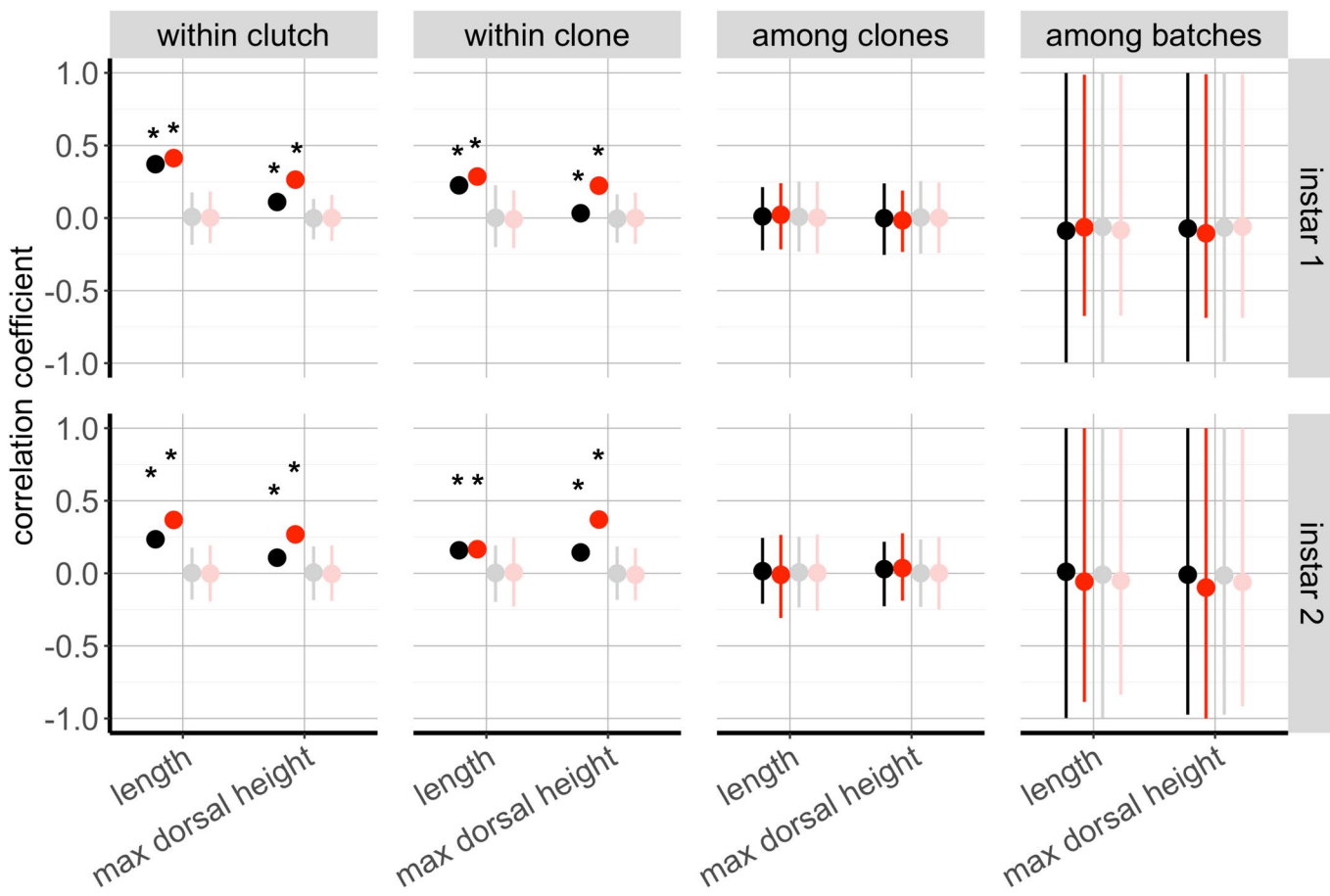




**Extended Data Fig. 6 | Effects of predation risk on morphological changes in genetically similar strains.** (A) Risk of predation induces plastic responses, with strongest phenotypic changes observed in the head region. (B,C) In response to predation, maximum dorsal height increases and shifts towards anterior head regions. (D) In addition, the number of neckteeth increases under predation risk. Notably, variation in morphological changes within genetically similar clones is as pronounced as that observed among genetically unique clones (see Fig. 2). (E) Effect sizes from analyses of variance along the dorsal shape reveal distinctive patterns of treatment (that is, predation risk, red line), genotype (blue line), and GxE (grey line) effects on morphological changes in second instar animals. (F) Broad-sense heritability estimates of dorsal height in second instar *Daphnia* vary along the dorsal axis in response to control conditions (black line) and predation risk (red line) in genetically similar strains. Data in panels E and F are presented as mean values, with shaded areas indicating upper (0.95) and lower (0.05) confidence intervals. Vertical lines highlight morphological independent shape modules, separating head and posterior body areas (see Extended Data Fig. 5).



**Extended Data Fig. 7 | Split-block experimental design.** Clonally related and genetically unique strains were phenotype concurrently across 20 experimental batches (A), with treatment conditions (control vs predation) relatively evenly split across batches (B). Note, due to technical failures, batches 2 and 3 were excluded from the experiment.



**Extended Data Fig. 8 | Genetic differences drive phenotypic variation in antipredator defences.** Phenotypic variation in genetically similar strains arises due to genetic effects: phenotypic responses (here: animal length and maximal dorsal height) of offspring released from the same mother ('within clutch') and same strain ('within clone') are more similar to each other than to offspring released from a randomly drawn member of the clonal assemblage ('among clones'). Correlation coefficients broadly exceed coefficients calculated for permuted data. Moreover, phenotypic correlations among randomly paired individuals from the same experimental batches are low, with actual data not exceeding permuted data ranges. Black and red points indicate control and predation risk conditions with darker and lighter colours depicting actual and permuted data, respectively. Data are presented as mean values, with error bars indicating upper (0.95) and lower (0.05) confidence intervals. Asterisks indicate actual data exceeding permuted data ranges (see Supplementary Table 1).

## Reporting Summary

Nature Portfolio wishes to improve the reproducibility of the work that we publish. This form provides structure for consistency and transparency in reporting. For further information on Nature Portfolio policies, see our [Editorial Policies](#) and the [Editorial Policy Checklist](#).

### Statistics

For all statistical analyses, confirm that the following items are present in the figure legend, table legend, main text, or Methods section.

n/a Confirmed

- The exact sample size ( $n$ ) for each experimental group/condition, given as a discrete number and unit of measurement
- A statement on whether measurements were taken from distinct samples or whether the same sample was measured repeatedly
- The statistical test(s) used AND whether they are one- or two-sided  
*Only common tests should be described solely by name; describe more complex techniques in the Methods section.*
- A description of all covariates tested
- A description of any assumptions or corrections, such as tests of normality and adjustment for multiple comparisons
- A full description of the statistical parameters including central tendency (e.g. means) or other basic estimates (e.g. regression coefficient) AND variation (e.g. standard deviation) or associated estimates of uncertainty (e.g. confidence intervals)
- For null hypothesis testing, the test statistic (e.g.  $F$ ,  $t$ ,  $r$ ) with confidence intervals, effect sizes, degrees of freedom and  $P$  value noted  
*Give P values as exact values whenever suitable.*
- For Bayesian analysis, information on the choice of priors and Markov chain Monte Carlo settings
- For hierarchical and complex designs, identification of the appropriate level for tests and full reporting of outcomes
- Estimates of effect sizes (e.g. Cohen's  $d$ , Pearson's  $r$ ), indicating how they were calculated

*Our web collection on [statistics for biologists](#) contains articles on many of the points above.*

### Software and code

Policy information about [availability of computer code](#)

Data collection

N/A

Data analysis

All scripts and code used for data analysis and plotting are available at <https://github.com/beckerdoerthe/SelectionPlasticity>. Our automated image analysis pipeline 'DAPCHA' is available at [https://github.com/beckerdoerthe/Dapcha\\_v.1](https://github.com/beckerdoerthe/Dapcha_v.1).

For manuscripts utilizing custom algorithms or software that are central to the research but not yet described in published literature, software must be made available to editors and reviewers. We strongly encourage code deposition in a community repository (e.g. GitHub). See the Nature Portfolio [guidelines for submitting code & software](#) for further information.

### Data

Policy information about [availability of data](#)

All manuscripts must include a [data availability statement](#). This statement should provide the following information, where applicable:

- Accession codes, unique identifiers, or web links for publicly available datasets
- A description of any restrictions on data availability
- For clinical datasets or third party data, please ensure that the statement adheres to our [policy](#)

All raw images and processed data used to generate figures are deposited in Zenodo (DOI 10.5281/zenodo.4738526). All sequencing reads are available from the Sequence Read Archive (PRJNA725506).

## Human research participants

Policy information about [studies involving human research participants and Sex and Gender in Research](#).

Reporting on sex and gender

N/A

Population characteristics

N/A

Recruitment

N/A

Ethics oversight

N/A

Note that full information on the approval of the study protocol must also be provided in the manuscript.

## Field-specific reporting

Please select the one below that is the best fit for your research. If you are not sure, read the appropriate sections before making your selection.

Life sciences

Behavioural & social sciences

Ecological, evolutionary & environmental sciences

For a reference copy of the document with all sections, see [nature.com/documents/nr-reporting-summary-flat.pdf](https://nature.com/documents/nr-reporting-summary-flat.pdf)

## Ecological, evolutionary & environmental sciences study design

All studies must disclose on these points even when the disclosure is negative.

Study description

This study examined genetic variation in predator induced morphological defenses in Daphnia pulex. This study involved sampling clones from a natural population, establishing them in the lab, and rearing them in a split-block design in the presence and absence of predator cue and measuring induction over 3-4 days per individual. Additional data were acquired via analysis of genomic material.

Research sample

The sample included 105 clonal strains of Daphnia pulex originally sampled from the Kilwood Nature Reserve in Dorset, England. The population was sampled because that locality had been used for previous work. The number of clones was chosen because that what was the largest sample size that we could manage experimentally. We collected data from 3-4 individuals per clone.

Sampling strategy

We measured 3-4 individuals per clone, and offspring were the daughters from two separate mothers per clone. We chose this number based on previous work, to manage and evaluate maternal effects as well as our treatments and because it was the largest replicate size that we could accommodate for the large sample size that we used.

Data collection

All Daphnia pulex samples were collected via standard procedures using plankton sampling tow nets. Samples were made at the the Kilwood Nature Reserve in Dorset, England. All phenotype data were collected at the University of Virginia using a mixture of multi-person observation (see reproducibility below) and semi-supervised automated image analysis. All genomic extractions were made at the University of Virginia using standard protocols. All sequencing were performed by....

Timing and spatial scale

Samples were collected in a single visit to all ponds in spring 2017.

Data exclusions

All samples were initially reared in a mix of natural pond water and artificial pond water and ultimately in 100% artificial ppnd water. The only data exclusions are represented by those samples not surviving this process.

Reproducibility

We developed an semi-supervised method to automatically score predator response and animal length. We verified that this method was repeatable and accurate using human manual measurements. All genomic data is available in open access repositories to allow re-analysis. A larger percentage of the clones are still in culture and available. All genomic extraction and analysis methods follow established pipelines described in the method section. All statistical code is available to re-create the analyses.

Randomization

For the experimental work, we used a randomized split-plot design.

Blinding

Blinding was not used. Instead, repeatability and replicability was formally assess among the network of observers and aligned with automated, semi-supervised scoring of the phenotype.

Did the study involve field work?

Yes       No

## Field work, collection and transport

Field conditions	Field conditions for collection were wet, approximately 10C and in March 2017, Dorset, UK.
Location	All Daphnia pulex samples were collected via standard procedures using plankton sampling tow nets. Samples were made at the Kilwood Nature Reserve in Dorset, England.
Access & import/export	All data collection was made with permission from the Dorset Wildlife Trust. They are acknowledged.
Disturbance	There was minimal disturbance to the habitat; sampling followed well established procedures using plankton tow nets. All sites were accessed by established paths.

## Reporting for specific materials, systems and methods

We require information from authors about some types of materials, experimental systems and methods used in many studies. Here, indicate whether each material, system or method listed is relevant to your study. If you are not sure if a list item applies to your research, read the appropriate section before selecting a response.

### Materials & experimental systems

- |                                     |                               |
|-------------------------------------|-------------------------------|
| n/a                                 | Involved in the study         |
| <input checked="" type="checkbox"/> | Antibodies                    |
| <input checked="" type="checkbox"/> | Eukaryotic cell lines         |
| <input checked="" type="checkbox"/> | Palaeontology and archaeology |
| <input checked="" type="checkbox"/> | Animals and other organisms   |
| <input checked="" type="checkbox"/> | Clinical data                 |
| <input checked="" type="checkbox"/> | Dual use research of concern  |

### Methods

- |                                     |                        |
|-------------------------------------|------------------------|
| n/a                                 | Involved in the study  |
| <input checked="" type="checkbox"/> | ChIP-seq               |
| <input checked="" type="checkbox"/> | Flow cytometry         |
| <input checked="" type="checkbox"/> | MRI-based neuroimaging |